REDUCED ILEUM PERISTALTIC CONTRACTILITY IN CYSTIC FIBROSIS SWINE

A Thesis Submitted to the College of Graduate and Postdoctoral Studies in Partial Fulfilment of Requirements for the Degree of Master in Anatomy, Physiology and Pharmacology (APP)

University of Saskatchewan

Saskatoon

Lingxiu Susan Liu

PERMISSION TO USE

In presenting this thesis/dissertation in partial fulfillment of the requirements for a Postgraduate degree from the University of Saskatchewan, I agree that the Libraries of this University may make it freely available for inspection. I further agree that permission for copying of this thesis/dissertation in any manner, in whole or in part, for scholarly purposes may be granted by the professor or professors who supervised my thesis/dissertation work or, in their absence, by the Head of the Department or the Dean of the College in which my thesis work was done. It is understood that any copying or publication or use of this thesis/dissertation or parts thereof for financial gain shall not be allowed without my written permission. It is also understood that due recognition shall be given to me and to the University of Saskatchewan in any scholarly use which may be made of any material in my thesis/dissertation.

Requests for permission to copy or to make other uses of materials in this thesis/dissertation in whole or part should be addressed to:

Head of the Department of Anatomy, Physiology and Pharmacology
Health Sciences Building, 107 Wiggins Road
University of Saskatchewan
Saskatoon, Saskatchewan S7N 5E5 Canada

Dean
College of Graduate and Postdoctoral Studies
University of Saskatchewan
116 Thorvaldson Building, 110 Science Place
Saskatoon, Saskatchewan S7N 5C9 Canada

ABSTRACT

Cystic fibrosis (CF) is an autosomal recessive multiorgan disease caused by mutations in the gene encoding for the Cystic Fibrosis Transmembrane conductance Regulator (CFTR). Even though CF-related lung diseases have traditionally been the main focus of both research and clinical concern, many extrapulmonary complications affect CF patient's quality of life. With the improvements in lung health and increases in the median age of survival for CF patients, extrapulmonary complications have gained increasing attention. Abdominal complications have been reported as the most common extrapulmonary diseases in CF patients. However, the research of the underpinning causes for these clinical presentations of CF is still evolving. This study focused on testing ileum peristaltic contraction between CFTR knockout ($CFTR^{-/-}$ or CF) and wild-type pigs as a model using the organ bath system. We tested the contractility of the ileum *ex vivo* in $CFTR^{-/-}$ and wild-type swine immediately after birth (i.e. neonates), when the animals do not display any lung disease, and in one-week-old animals that start to develop signs of lung disease. We measured basal ileum peristalsis and the contraction induced by the agonists, acetylcholine, serotonin, and histamine. We then found that, in general, contraction in the CF ileum decreased compared to wild-type ileum right at birth and did not improve a week later. Moreover, CF pig ileum responded with a lower maximum contraction after stimulation with acetylcholine. The results support the hypothesis that the dysfunction of the CFTR channel results in reduced contraction. We hypothesize that the peristaltic contraction defect may be at the level of the intestinal smooth muscle.

ACKNOWLEDGEMENT

I am very thankful to have the opportunity to do a one-year Master's with my wonderful supervisor Dr. Juan Ianowski researching a new area about Cystic Fibrosis. I am grateful that Dr. Ianowski accepted me as his honour's student back in March 2019 when I was stressed to find a supervisor for my honours project for my undergraduate program. It was such an honour and exceptional experience to work with Dr. Ianowski about CF. Thank you so much for providing the resources for my experiments and giving me insight about what to analyze when I didn't know what to do. You are a great researcher! It was such an honour to be your student!

I would like to thank my committee members, Dr. Kash Desai and Dr. Veronica Campanucci. I would like to thank Dr. Desai for supporting me when I was conducting the organ bath experiment. Thank you for letting me use the organ bath apparatus and teaching me how to properly use the apparatus. I am grateful to have you as my committee member. I want to thank my committee chair Dr. Veronica Campanucci for hosting all the meetings, letting me use some of your equipment, and giving me feedback for my experimental results. I also want to thank CoMGrad for funding this research.

I want to thank Nicolas Romero and Raina Kim for conducting the organ bath experiment for the CF tissues. Thank you both for staying up late and waiting for the pigs to give support for my experiment. I also want to thank Dr. Xiaojie Luan and Dr. Emma Le for their support in the lab.

I want to thank my parents and my church family for their support and prayers during my school year. Your love really encouraged me. I wouldn't have finished this without your support.

Lastly, I want to give thanks and glory to my God and Lord Jesus Christ for how you have saved me and the wonderful works you have done in my life. Truly, you work all things together for good for those who are called according to your purpose. Praise your name!

"Great are the works of the LORD, studied by all who delight in them. (Psalm 111: 2)"

TABLE OF CONTENT

LIST OF TABLES

LIST OF FIGURES

LIST OF ABBREVIATIONS

ACh - Acetylcholine

CF - Cystic Fibrosis

CFTR - Cystic Fibrosis Transmembrane conductance Regulator

CNS - Central Nervous System

DIOS - Distal Intestinal Obstruction Syndrome

DR - Dose Ratio

ENS - Enteric Nervous System

EC_{50} - Effective Concentration at half maximal response

Emax - Maximal response

GI - Gastrointestinal

MI - Meconium ileus

MLCK - Myosin Light Chain Kinase

PKA - Protein Kinase A

PKC - Protein Kinase C

VIP - Vasoactive intestinal peptide

CHAPTER 1. BACKGROUND

1.1 Cystic Fibrosis

1.1.1. Introduction

Cystic Fibrosis (CF) is an inherited autosomal recessive fatal multiorgan disease [1] that affects 70,000 to 100,000 people worldwide, and there are approximately 1000 new cases diagnosed every year [2]. The cause of CF is mutation in the Cystic Fibrosis Transmembrane conductance Regulator (CFTR) gene, located on chromosome 7. The CFTR protein is an anion channel expressed in different parts of the body, including the lungs, gut, pancreas, and sweat glands. The CFTR protein contributes to regulating chloride and bicarbonate transport in epithelial cells and intracellular Cl^- homeostasis in neurons and muscle cells [3]. All organs that normally express CFTR are compromised in cystic fibrosis patients.

Even though it is not clear when CFTR mutations first appear in the human genome, there seem to be references to CF in European folklore since the middle ages [4]. However, CF was scientifically first described and identified as a distinct disease in 1938 by Dorothy Andersen in malnourished infants [5]. She described the presence of mucus plugging of the glandular ducts and named the disease "Cystic Fibrosis of the pancreas" [5–7]. Later the disease became known as a "generalized exocrinopathy" as exocrine glands are affected by thick mucus. In 1948, Dr. Paul di Sant'Agnese, a pediatrician in New York, found that infants arriving at his practice with heat prostration during a heatwave had a very high prevalence of CF. He then tested the CF patient's sweat and discovered that it had five times more NaCl than a healthy individual [8]. In 1983, Paul Quinton, himself a CF patient, used his own sweat gland ducts to study the pathophysiology of CF and identified abnormal Cl^- transporter as the basic defect in CF, giving the first indication that CFTR may be a Cl^- channel [9].

In 1989, Drs. Lap-Chee Tsui and John Riordan found the gene that encodes for CFTR while working at "Hospital for SickChildren" in Toronto, Canada [10,11]. Trikafta, the first highly effective treatment for most CF patients, was approved for human treatment in 2019 in the US and 2021 in Canada [12]. The future looks brighter for CF patients after a long journey that

transforms the expected median age of survival of just a few months in the 1950s to ~50 years in 2020 in Canada. Furthermore, thanks to the new highly effective treatments, the life expectancy and quality of CF patients will continue to improve [13,14].

Due to the increase in the age expectancy of CF patients, CF related complications other than the life-threatening lung disease are now beginning to be the subject of intense research [15]. Gastrointestinal complications that can severely affect the day-to-day life of CF patients and causing pain. For this thesis, we tested the hypothesis that CF gastrointestinal tract suffers from abnormal gastrointestinal motility that may contribute to constipation, distal intestinal obstruction syndrome and pain.

1.1.2 Molecular structure and function of CFTR

The Cystic Fibrosis Transmembrane conductance Regulator (CFTR) channel is part of the ATP-binding cassette (ABC) protein family, which are predominantly active ion transporters [16]. However, CFTR is the only known ABC protein that acts as an anion channel permeable to Cl^- and HCO_3^- [17,18].

CFTR contains two transmembrane domains (TMDs) and two nucleotide-binding domains (NBDs), a regulatory domain (R), and long N- and C-terminal extensions [10,18](*Figure 1-1*). Each of the two TMDs of the CFTR contains six membrane-spanning alpha-helices on the phospholipid bilayer, thus forming a pore for the passage of anions [19,20]. The NBDs contain an ATP binding site [21]. Lastly, the R domain of the CFTR is highly charged and contains consensus sequences for the cAMP-dependent protein kinase A (PKA) and protein kinase C (PKC) phosphorylation required for the opening of the CFTR channel [18,21].

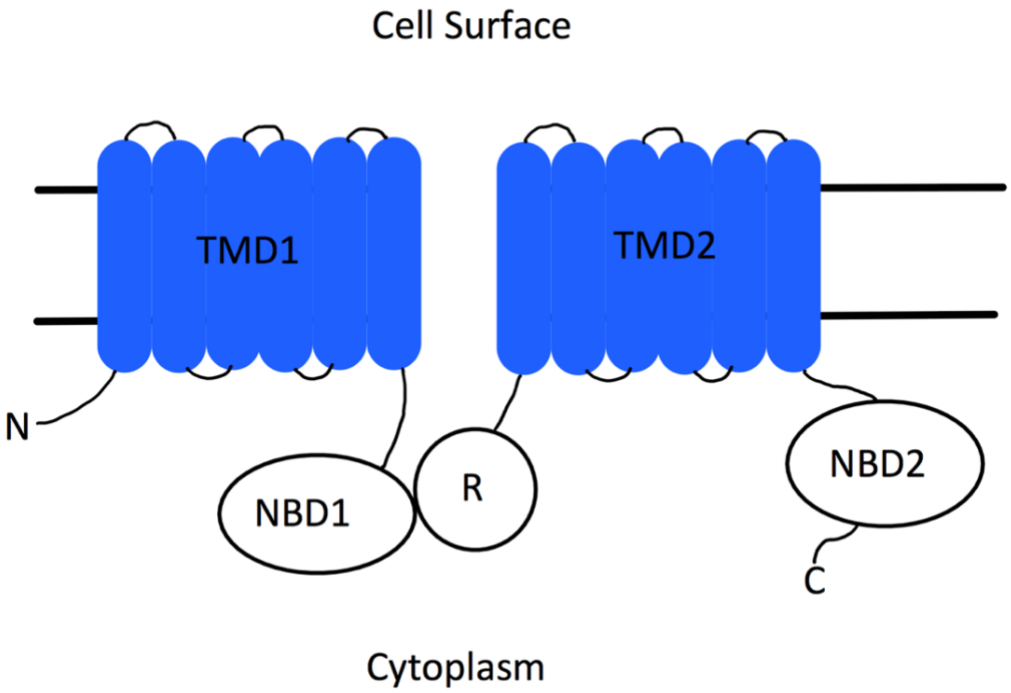

Figure 1-1: The structure of CFTR. The protein includes an N-terminus, two transmembrane domains (TMD1 and TMD2), two nucleotide-binding domains (NBD1 and NBD2), the regulatory domain (R), and a C-terminus [18,21].

At resting state, the R domain is dephosphorylated and it interacts with the NBDs which prevent ATP binding [16]. At this point, the R domain acts as an inhibitor to the CFTR channel [21]. Studies have shown that CFTR channels with the deleted R domain are constitutively open. The inhibitory effect of the R domain can be removed through phosphorylation by PKA and PKC [22]. Phosphorylation decreases the interaction of the R domain with the NBDs and increases its interaction with the C terminus. The NBDs are then free to bind to ATPs and initiate the opening of the channel. When ATP bind to both NBDs, they form a head-to-tail sandwich heterodimer. The dimer then causes the conformational change of the TMDs resulting in the opening of the channel [18,23]. The channel opening allows the diffusion of anions passively down its concentration gradient [16,20,24,25]. NBDs then hydrolyze the bound ATP to ADP and Pi causing dimer destabilization and eventually the closing of the channel [18,21] (*Figure 1-2*).

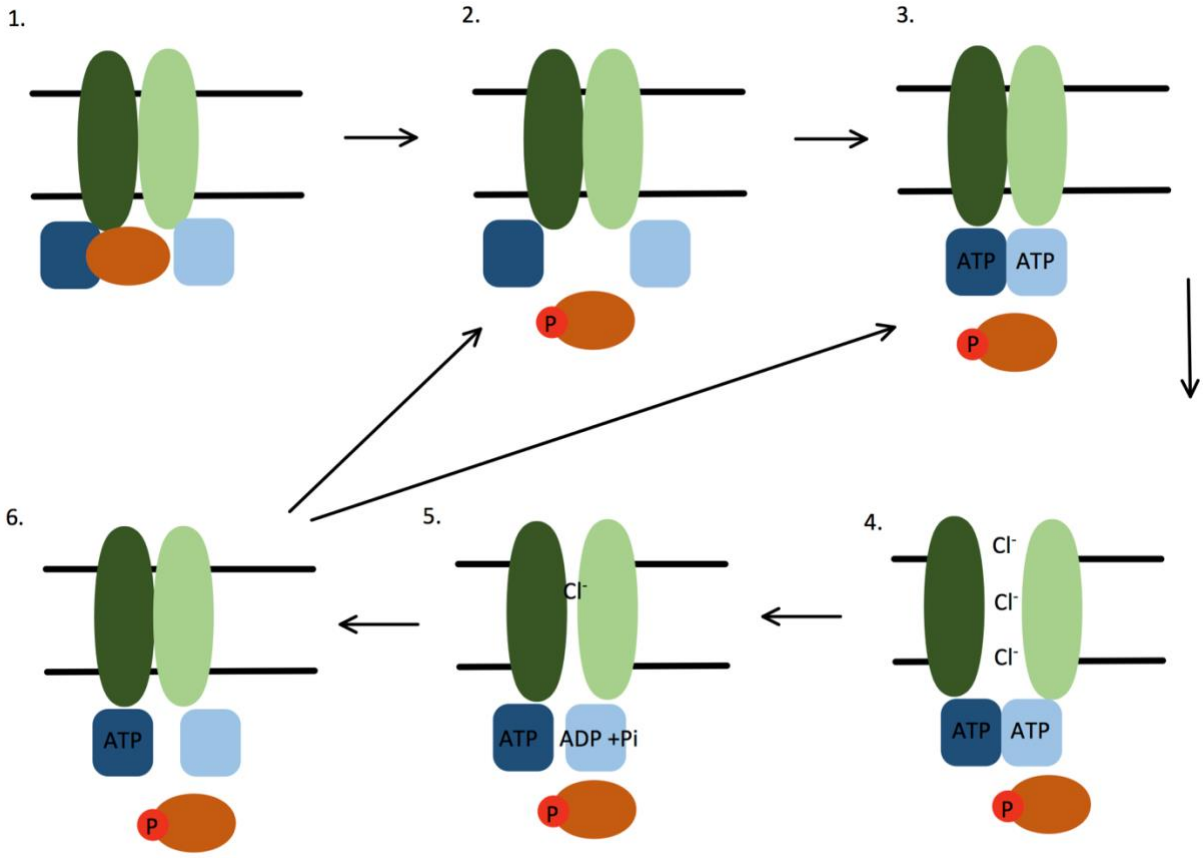

Figure 1-2: The mechanism of CFTR opening and closing. The two green oval circles represent the TMDs (the dark green circle as TMD1 and the light green circle as TMD2). The two blue squares represent the NBDs, with the dark blue square as NBD1 and the light blue square as NBD2. The orange oval circle is the R domain. When the red dot labeled with "P" is attached to the R domain, it indicates that the R domain is phosphorylated. 1) The channel at resting state with the pore closed, NBDs detached from each other, and the R domain dephosphorylated and interacting with the NBD1. 2) Phosphorylation of the R domain by PKA and/or PKC leads to the disruption of the interaction with NBD1. At this stage, the NBDs are free to bind ATP. 3) ATP binds to the NBDs and form a head-to-tail heterodimer. The channel at this point is in the open-ready transition conformation, where the channel is still closed but ready to open. 4) Dimerization of the NBDs causes the conformational change of the TMDs, results in the opening of the channel and anions passage through the pore. 5) The dimer is destabilized due to the hydrolysis of ATP to ADP plus Pi, and then the channel closes. 6) ATP may still bind to the NBDs, which allows the channel to quickly go back to the open-ready transition conformation. The figure was drawn based on [18].

1.1.3 Genetic basis of CF

CF is caused by mutations in the Cystic Fibrosis Transmembrane conductance Regulator (*cftr)* gene. The *cftr* gene is approximately 6500 nucleotides in size, 250kB in length that encodes for the 1480 amino acids CFTR protein [7]. Since the identification of the cftr gene in 1989, over 100 reported disease-causing mutations have been reported [10,26]. These mutations are classified into six different classes based on the type of mutations and biological effects [26] (*Figure 1-3*).

Class I mutations arise due to frame-shift mutations, nucleotide substitution, complete or partial deletion of the CFTR gene, and rearrangement in the gene-altering exon sequence. These mutations result in a total or partial lack of *cftr* gene transcription [26,27]. Class II mutations are associated with defective intracellular processing of the CFTR and trafficking to the cell membrane. The misfolded CFTR protein is detected by the quality control mechanism in the endoplasmic reticulum and targeted for proteasomal degradation [28–30]. The most common CFTR mutation is class II mutation that consists of a deletion of a phenylalanine in position 508 (F508del). This mutation is carried by around 90% of CF patients with around 70% of the patients being homozygous for this mutated allele [31]. Class III mutation, often known as the "gating mutations", affects the ATP binding domains, the NBD1 and NBD2 [27]. These mutations can produce proteins that insert into the cell membrane but cannot be activated by phosphorylation[32]. Class IV mutation affects the membrane-spanning protein. The production and insertion of the protein are normal, but the conduction of the channel (or channel opening) is greatly reduced [27,33]. Class V mutation affects pre-mRNA splicing and splicing site that results in the complete or partial exclusion of exons. It results in a reduced amount of functioning CFTR protein [27]. Class VI mutation reduces the conformational stability of the CFTR channel post-endoplasmic reticulum compartment or at the plasma membrane. This increases the plasma membrane turnover and reduces the expression of the CFTR protein [26].

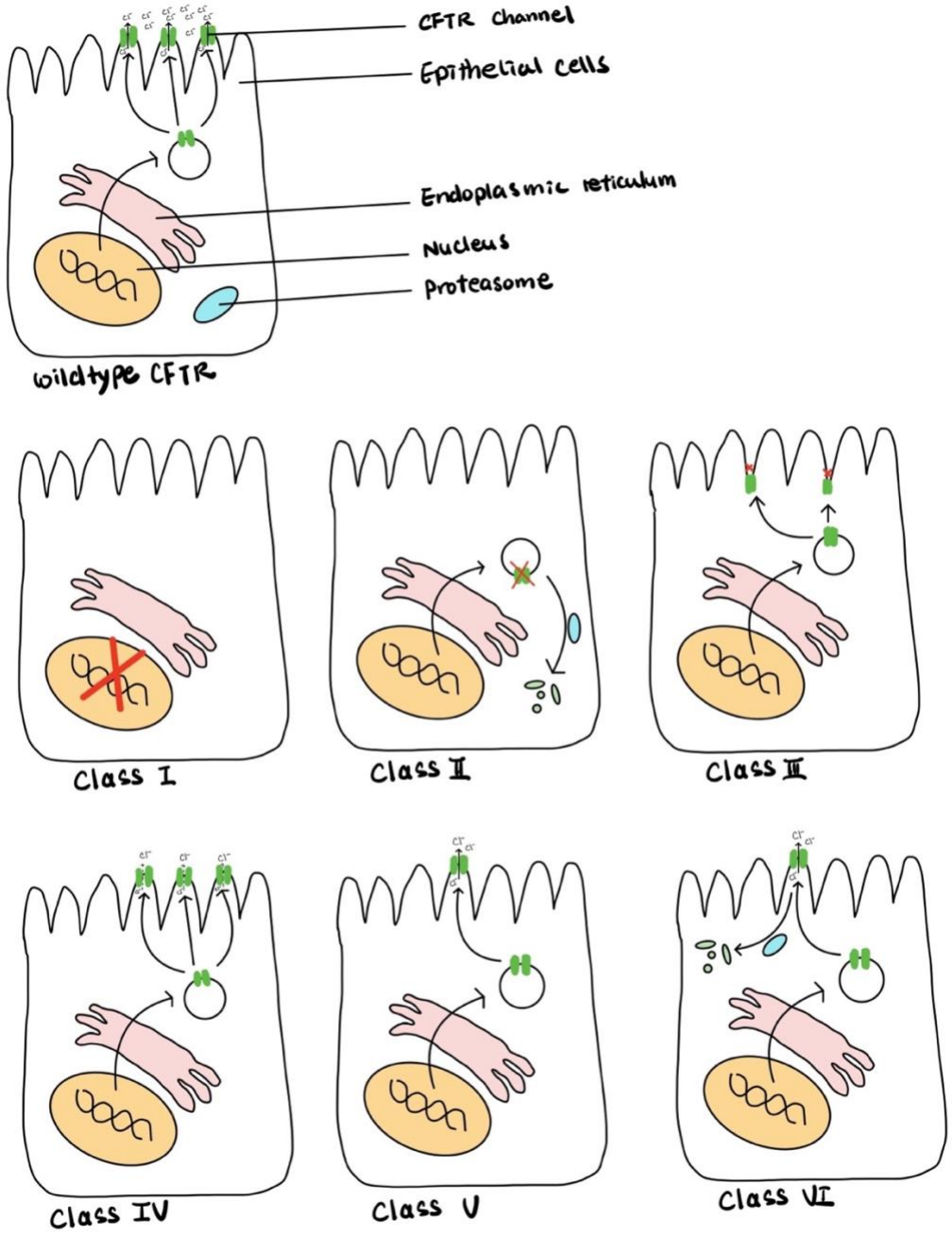

Figure 1-3: Illustration of the six different classes of CFTR mutations. The yellow circle represents the nucleus, the pink shape represents the endoplasmic reticulum, the blue circle is the proteasome, and the CFTR channel is in green. Class I, synthesis defect; Class II, maturation defect; Class III, gating defect; Class IV, conductance defect; Class V, reduced quantity; Class VI, reduced stability. The image is modified based on [26,27].

1.1.4 Pathology and symptoms of CF

CFTR is expressed in many organs and tissues in the body, including the respiratory, pancreas, nervous, and gastrointestinal systems. Even though all the systems that normally express CFTR are compromised in CF, most of the morbidity and mortality have traditionally been associated with lung complications. The loss of CFTR function in the lungs affects the ability of the airway to clear inhaled pathogens due to the reduction of antimicrobial properties of the airway and the malfunction of the mucociliary clearance apparatus that traps, kills, and clears pathogens. Thus, CF patients are more susceptible to airway infections inflammation that may eventually result in airway remodeling, respiratory failure, and death [24].

Dysfunctional CFTR protein also affects the digestive system by affecting gastrointestinal ion and fluid transport, as well as affecting the liver, pancreas, and gall bladder [7,34,35]. CF patients can also have abnormalities in the nervous system and muscle tissue that play a role in gastrointestinal function [36]. However, the contribution of neuronal or muscle abnormalities due to CFTR to the gastrointestinal complication is not understood. The lack of knowledge makes it difficult to improve the quality of care for gastrointestinal complications [37,38].

1.2 Gastrointestinal physiology and motility

1.2.1 General GI physiology

The gastrointestinal (GI) system is responsible for the effective digestion and absorption of food [39,40]. The human GI tract starts from the mouth, where food enters and ends in the anus, where wastes get excreted. The organs that made up the GI system are the mouth, esophagus, stomach, small intestine, large intestine, rectum, and anus. The mouth, esophagus, stomach, and small intestine are considered the upper GI tract. The large intestine, rectum, and anus are the lower GI tract. The small intestine can also be further divided into three subsections, the duodenum, jejunum, and ileum [40].

Food contents usually move along the GI tract through the periodic contraction of smooth muscle lining the GI tract. Smooth muscle contraction may generate two different contraction

patterns, segmentation, and peristalsis. Segmentation in GI contractions ensures the contents get mixed, fully digested, and absorbed, while peristaltic contraction drives the food contents along the GI tract [40]. These coordinated digestive events in the GI tract are facilitated by the Central Nervous System (CNS) as well as the Enteric Nervous System (ENS) intrinsic to the gut [40]. ENS innervation is considered intrinsic while CNS innervation is extrinsic through vagus and splanchnic nerve innervations. The roles of the ENS includes determine the movement pattern, control secretion, regulate fluid movement, change local blood flow, modify nutrient handing, and interaction with immune and endocrine system of the gut[41].

The CFTR protein is expressed both in smooth muscle and in the nervous system [42]. Thus, we would expect that in CF tissues the motility of the GI tract may be compromised, and the transit of the contents may be slower than normal, potentially contributing to GI blockage as well as malabsorption of nutrients.

1.2.2 GI motility and CF-related GI motility complications

1.2.2.1 Intestinal motility physiology

Intestinal motility is an integrated process under the control of the CNS, ENS, hormones, and paracrine agents, and the intestinal cells of Cajal which modulate muscle tone and contractility by setting up the pace for spontaneous electric waves that spread through the smooth muscle [39,40,43]. The intestinal cells of Cajal connect not only to muscles cells but also nerve terminals and each other. Different neuronal humoral substances can influence this pacemaker[43]. There are inhibitory receptors for nitric oxide and excitatory receptors for muscarinic agonists. The intestinal cells of Cajal can initiate slow waves and spike potential if excited by agonists[43].

The small intestinal wall contains muscularis externa and muscularis mucosa. The muscularis mucosa can be divided into two cell layers, the inner circular smooth muscle layer and the outer longitudinal smooth muscles layer. The longitudinal smooth muscle is perpendicular to smooth muscle and has a thinner layer with lesser innervations. The circular layer can mediate basic contractile patterns (slow waves) while the longitudinal layer could not but function to accelerate transit times[44]. The laminar septae separate longitudinal and circular

layers into bundles of contractile units. The smooth muscles are embedded in the connective tissue matrix where different structures such as intestinal cells of Cajarglial cells and fibroblasts. The muscularis mucosa is involved in secretion[44].

The GI smooth muscles are unitary with coordinated contraction to act as a single unit. There are caveolae and dense bands located on the smooth muscle membrane. First, the caveolae have basket-shaped structures and store calcium ions. Second, the dense bands separate the caveolae and thin actin filaments attached to them. Furthermore, dense bodies in the cytoplasm and dense bands on the membrane are linked by intermediate filaments to transmit the generated muscle contraction from within the cell[43]. There are also gap junctions mostly on the circular smooth muscle layer that allow propagation of intracellular molecules such as calcium ions[45]. The intestinal cells of mesenchymal origin that form the intestinal cells of Cajal are also the origination of these gap junctions [44].

Smooth muscles in the intestine are connected by electrical and mechanical junctions. These junctions create uniform and synchronized contractions during peristalsis and segmentation [46]. The longitudinal and circular smooth muscles contract and relax opposite to each other and create peristaltic waves to propel the chyme down the GI tract. Instead of propagating along the entire intestine, the peristaltic wave created by both types of smooth muscles can only move the chyme a few centimeters [47]. Along with neuronal innervation, smooth muscles are integral in intestinal motility.

1.2.2.2 Smooth muscle contraction mechanism

The contraction of smooth muscle starts with the release of Ca^{2+} into the cytosol of the cell. There are three different ways that Ca^{2+} enters the cytoplasm of the smooth muscle cell. First, there are voltage-dependent Ca^{2+} channels. With depolarization of the smooth muscle cell membrane and the generation of the action potential, these Ca^{2+} channels are opened which increases the intracellular Ca^{2+} level [48]. Second, the activation of metabotropic receptors, such as muscarinic ACh receptors, that stimulate intracellular second messenger pathway and the activation of non-selective Ca^{2+} channels [46,49]. And third, Ca^{2+} release from intracellular storage

such as the sarcoplasmic reticulum (SR) is through the activation of receptors expressed on the SR membrane, including ryanodine receptors and inositol 1,4,5-triphosphate (IP_3) receptor [50,51]. The ryanodine receptor is activated by the increase in intracellular Ca^{2+} level, through a mechanism called Ca^{2+}-activated Ca^{2+} release. The opening of the IP_3 receptors is activated by IP3 produced by the action of phospholipase Cβ (PLCβ) [46].

Cytosolic Ca^{2+} ions can bind to calmodulin and activate the Myosin Light Chain Kinase (MLCK). The activation of the Ca^{2+}/Calmodulin dependent MLCK phosphorylates the 20kDa myosin light chain and initiates the interaction between myosin and actin and the muscle contraction cross-bridge cycling [48,52]. Different from contraction in skeletal and cardiac muscle, which is activated by uncovering the tropomyosin on actin, smooth muscles focus on activating myosin [53](*Figure 1-4*).

Some smooth muscles have an intrinsic tone, which is maintained by the phosphorylation of the myosin light chain without any external stimulus [53,54]. The intensity of this intrinsic tone can vary between smooth muscles in different organs of the body [53]. Constant peristalsis before adding any neurotransmitters in the gut can be considered as an intrinsic tone.

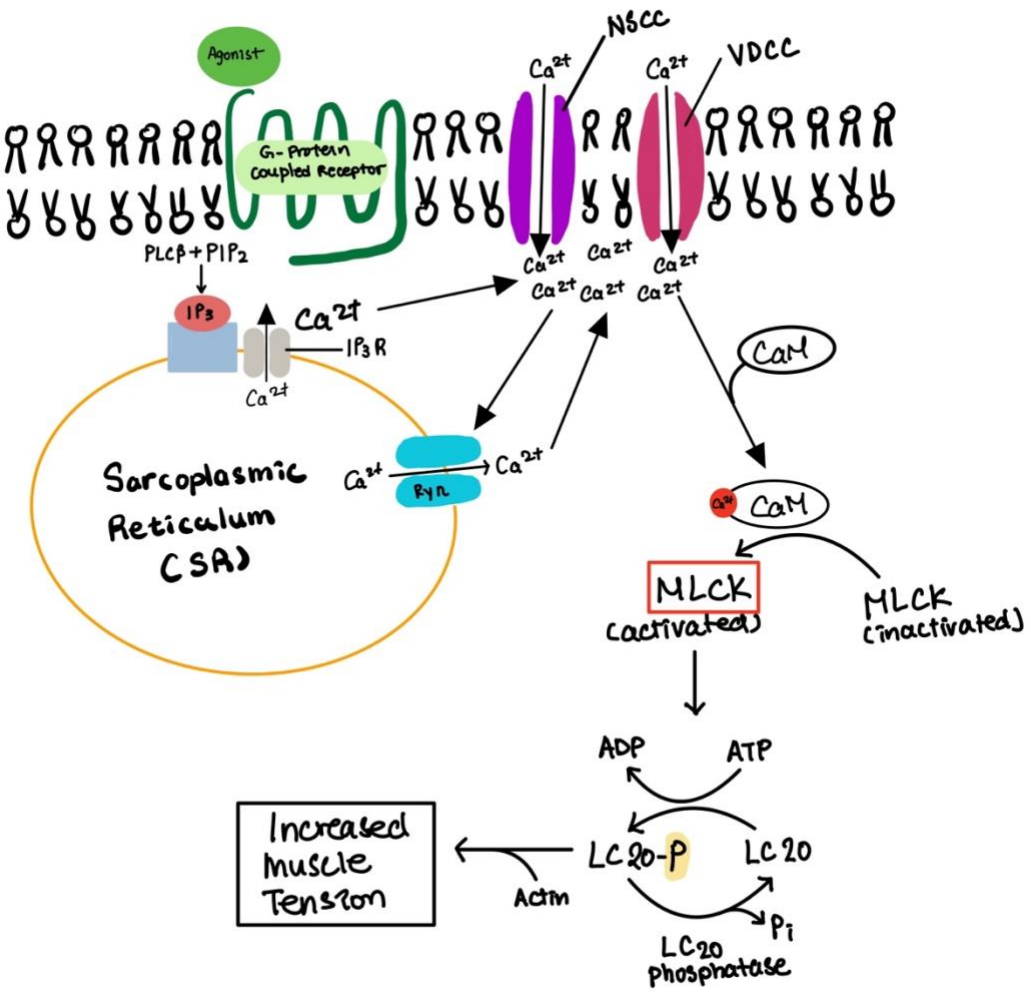

Figure 1-4: Diagram of the mechanism of smooth muscle contraction. PLCβ, phospholipase Cβ; PIP_2, phosphatidylinositol 4,5-bisphosphate; PC, phosphatidylcholine; IP_3, inositol 1,4,5-trisphosphate; IP_3R, inositol 1,4,5-trisphosphate receptor; SR, sarcoplasmic reticulum; MLCK, myosin light chain kinase; CaM, calmodulin; RyR, ryanodine receptor; LC_{20}, 20-kDa myosin light chain; The figure was drawn based on [52] *and* [46].

1.2.2.3 Neurohormonal innervation of the GI tract

Neuronal innervations are one of the integral components that control the GI system. The ENS is part of the peripheral nervous system subdivisions of the ANS intrinsic to the GI and specially organized to control smooth muscle and mucosal functions of the gut [40,55]. The roles of ENS in the GI systems are multiple and it includes establishing the pattern of movements of the GI tract. In contrast to esophageal and gastric segments of the GI tract where the control of

contraction is heavily dependent on the CNS. The medulla oblongata innervating the striated muscles primarily controls the esophageal propulsion. Similarly, the neuronal control of the stomach depends on vasovagal reflexes. On the other hand, ENS is the dominant control in the small and large intestine motility[41].

The ENS consists of nerve cells, enteric ganglia, neural connections between ganglia, and nerve fibers. ENS has ganglionated plexuses that are embedded between layers of the intestine that control different reflexes[44]. For medium-large mammals, the myenteric plexus is between the longitudinal and circular smooth muscle layers. The deep muscular plexus, outer and inner submucosal plexus are under the circular muscle layer in the submucosal layer. There are also vasculatures accompanying. These plexuses innervate the longitudinal muscle, circular muscle, muscularis mucus, intrinsic arteries, and mucosa[41].

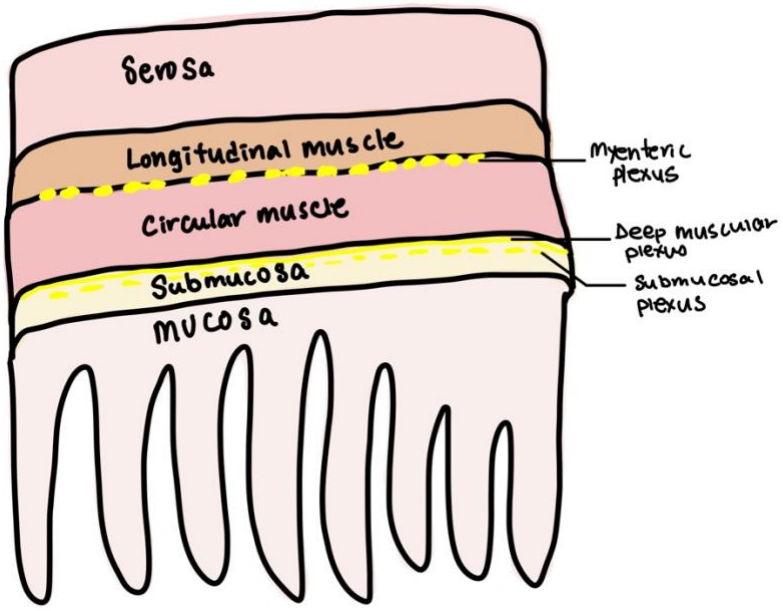

Figure 1-5: Diagram of the organization of the ENS in the intestine[41].

There are excitatory and inhibitory motor neurons, intrinsic sensory neurons, and interneurons in the ENS[56]. Since the dominant stimulatory pathway of the GI tract is parasympathetic, acetylcholine (ACh) is the main excitatory neurotransmitter for gut motility, however, there are other neurotransmitter receptors present that may play a role [55,57]. Other

excitatory neurotransmitters include substance P, serotonin, and histamine, while the major inhibitory neurotransmitters include vasoactive intestinal peptide (VIP) and nitric oxide (NO)[58]. The neurotransmitter substance P has a high concentration in the brain and spinal cord. It is also involved in inducing smooth muscle contraction by the ENS. It is in charge of modulating intestinal longitudinal muscle motor activity. The site of action of substance P is directly on muscle cells[59]. This explains why it is more potent than ACh and resistant to atropine. In the intestine, substance P levels are low in the esophagus and stomach, high in duodenum and jejunum and moderate in the ileum and large intestine[59].

Hormones also play an important role in modulating GI motility, including motilin and cholecystokinin[44]. Motilin is secreted from endocrine Mo cells found in the crypts of the small intestinal mucosal epithelium. Upon secretion, it stimulates intestinal contractility and regulates motility[44]. Motilin exerts its function through G protein-coupled receptors located on the ENS and intestinal smooth muscles. After the activation by motilin, the G protein-coupled receptor stimulates phospholipase C, thereby increasing intracellular Ca^{2+} release, which excites smooth muscle contraction[60]. Even though cholecystokinin is mainly involved in gall bladder emptying, it can also increase intestinal mobility. It is produced by enteroendocrine cells (I cells) in the small intestine and specialized neurons in the myenteric plexus[61]. Cholecystokinin exerts its function through the binding of G-protein coupled CCK-1 receptors. Other stimulatory hormones include gastrin-releasing peptide[44].

There are also important inhibitory neurohormones such as VIP and NO. VIP is a gut peptide hormone that acts on VPAC1 and VPAC2 receptors[62]. The VPAC1 receptor is the main receptor used by VIP in the GI system[63]. VPAC1 initiates G-protein stimulated Ca^{2+} to inflex to induce smooth muscle relaxation. VIP can also activate calmodulin-bounded nitrate oxide synthase (eNOS) to generate NO for further smooth muscle relaxation[64].

Table 1-1: Stimulatory and inhibitory signaling on intestinal motility[44].

Stimulatory	Inhibitory
Acetylcholine	Calcitonin gene-regulated peptide (CGRP)
Bombesin	Gamma butyric acid (GABA)
Cholecystokinin	Glucagon
Gastrin-releasing peptide (GRP)	Nitric oxide (NO)
Motilin	Secretin
Serotonin	Somatostatin
Substance P	Vasoactive intestinal polypeptide (VIP)

1.2.2.4 Intestinal Neurotransmitters

Acetylcholine

In the GI system, the release of ACh induces peristaltic movement by intestinal smooth muscle contraction [65] ACh is released from the vagus nerve and the pelvic splanchnic nerves. The neurotransmitter binds to membrane receptors, thus stimulating the postsynaptic membrane.

There are two basic types of ACh receptors, nicotinic and muscarinic. The nicotinic cholinergic receptors (nAChR) are ligand-gated ionotropic receptors. The muscarinic cholinergic receptors (mAChR) are G-protein coupled receptors (metabotropic receptors) and have a slower response compared to nicotinic receptors. Ligand binding leads to the activation of G-protein, which will subsequently activate a second messenger pathway that mediates other cellular responses [66]. The nAChRs are more commonly found in the neuromuscular junction of the skeletal muscles [55], while mAChR are found mostly in the smooth and cardiac muscles. Therefore, mAChR plays a more important role in intestinal smooth muscle contraction [67]. There are five known mAChRs (M_1-M_5) that are distributed along the small intestine. To induce a contraction of the intestine, acetylcholine acts on the M_2 and M_3 in the longitudinal muscle [68,69] (*Table 1-2*).

Table 1-2: Functions of M_1-M_5 receptors in the intestine [70](mAChR -muscarinic acetylcholine receptor).

mAChR 1	- Regulates IL_2 production in lymphocytes - Stimulates CD_8^+ differentiation
mAChR 2	- Regulate actions of acetylcholine
mAChR 3	- Contractility of the gastrointestinal tract - Smooth muscle relaxation by nitric oxide (NO) release
mAChR 4	- Regulate actions of acetylcholine
mAChR 5	- Associated with growth and proliferation of cancerous cells

Serotonin

Serotonin (5-hydroxytryptamine or 5-HT) is a major neurotransmitter in the human body, and roughly 95% of the 5-HT receptors are found in the gut [71]. The enterochromaffin cells (EC) in the intestinal mucosa are in charge of synthesizing serotonin [71] (*Figure 1-6*). 5-HT receptors are G-protein coupled receptors that can stimulate intrinsic reflexes that initiate and modifies motility, secretion, and vasodilation of the gut [40,72,73]. $5HT_3$ and $5HT_4$ receptors in the gut can facilitate both peristalsis and segmentation. However, $5HT_3$ plays a more important role in gut motility while the $5HT_4$ receptor is also in charge of stimulating Cl^- and water secretion [71,74]. $5HT_3$ antagonists and $5HT_4$ agonists can be used to treat diarrhea and constipation, respectively[72]. It has been suggested that serotonin usually acts on the longitudinal muscle in the distal ileum [75]. The increase in contraction through the $5HT_3$ receptor is mediated through a cholinergic pathway[76].

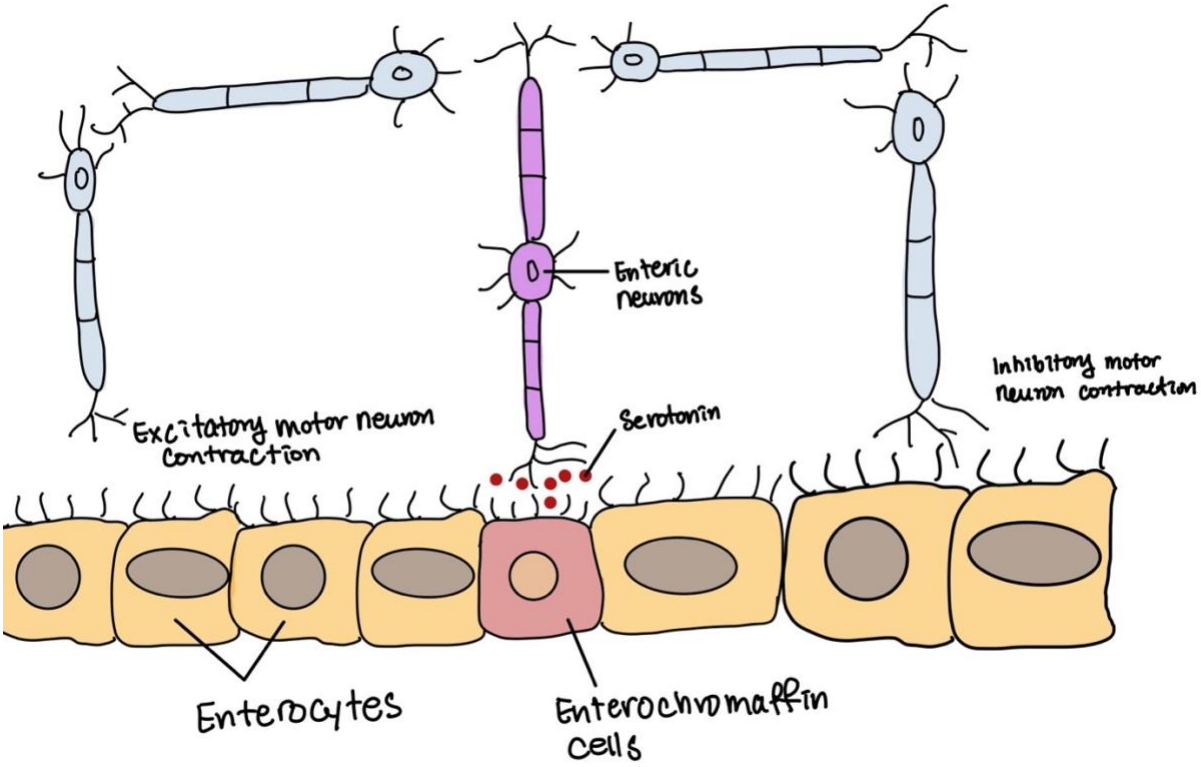

Figure 1-6: Serotonin released by enterochromaffin cells activates afferent enteric neurons which activates excitatory and inhibitory motor neurons for contraction and relaxation, respectively. Image was drawn based on [71].

Histamine

Histamine is produced in mast cells or EC via the decarboxylation of histidine and stored in the intracellular vesicles for later use [77]. There are four different histamine receptors found in the body which are H_1, H_2, H_3, and H_4, and they are present in different parts of the digestive system [77]. All four of them are G-protein coupled receptors. Histamine can bind to different receptors to induce different motility actions. In the gastrointestinal tract, histamine has three functions; gastric acid production, smooth muscle motility, and mucosal ion secretion [78]. Among the four discovered histamine receptors, H_1 induces smooth contraction in the airway and gastrointestinal tract, while H_2 regulates gastric as well as intestinal secretion [77,79].

1.2.2.5 CFTR function in the smooth muscle cell

CFTR is expressed on smooth muscle cells and there is evidence that it may function as a Cl^- channel and may affect the membrane potential [17]. CFTR modulates histamine-induced intracellular Ca^{2+} release in airway smooth muscle [80] and plays a role in the function and phenotype formation of the ileal smooth muscle [81,82]. CFTR may also contribute to the GI response to other stimulatory signals (e.g. cholinergic or serotonergic) which may fail in CF. Therefore, CFTR-related smooth muscle dysfunction may lead to gastric dysmotility and intestinal obstruction in CF [17].

1.2.2.6 CF-related GI complications

Meconium Ileus

Meconium is a dark green substance that is the first feces of the newborn. Meconium ileus (MI, ileus means lack of peristalsis) is a condition where the first stool of a newborn obstructs the GI tract. MI is one of the first symptoms observed in CF with an occurrence of up to 20% of CF patients [24,83,84]. Since MI occurs early in life, research has suggested that its development is more dependent on the genetic background of the patients rather than environmental factors. For instance, patients with class III mutation have lower risks of developing MI compared to those with class I or II mutations [85].

MI can be clinically classified into simple or complex [85,86]. Simple MI is the failure of passing meconium within 48 hours without other complications, while complex MI is the addition of other complications, which may result in meconium cysts and rupture [86]. Treatment of MI includes surgical removal or using osmolytes to draw fluid into the intestine [86,87]. Unfortunately, MI can also cause long-term abdominal abnormalities such as gut motility issues, meconium plug syndrome, colonic atresia, and rectal prolapse [85,86].

Distal Intestinal Obstruction Syndrome (DIOS)

Distal Intestinal Obstruction Syndrome (DIOS) was first described in 1945, and it is a syndrome of post-neonatal distal small bowel obstruction due to stool plugs [88]. DIOS has

traditionally been explained as the consequence of abnormal fluid secretion and increased viscosity of intestinal mucus [89]. However, the lack of intestinal movement could be a contributing factor. The prevalence rate of DIOS is around 10% to 24% in CF adult patients [34]. The obstruction from DIOS usually occurs in the distal small bowel and ileocecal junction. Through abdominal radiography, it was also found that fecal mass usually appears at the right lower quadrant of the intestine with a granular and bubbly appearance [85]. In contrast to MI, several studies have shown that the risk of developing DIOS correlates primarily with nongenetic factors [87].

DIOS can also be classified into two classes, partial or complete obstruction. A luminal osmotic agent may be able to relieve the partial obstruction while more complicated methods, including surgical interventions, are sometimes needed to clear the complete obstruction [85].

Constipation

Constipation is an infrequent bowel movement and is usually combined with abdominal pain and distension. The prevalence of constipation in CF patients is around 47%. This complication can generally be improved through medical interventions [90]. The main cause seems to be prolonged transit time and the alteration of intestinal fluid composition caused by the mutated CFTR [90,91].

Intussusception

Intussusception is a GI manifestation where one part of the intestine slides into another, which causes abdominal pain [34,85]. Intussusception occurs in around 1% of CF patients and is more common in older patients [34]. CF patients also have a 10 to 20 times higher rate of getting intussusception compared to the general population [85]. The majority of intussusception is ileocolic, and it is associated with small bowel obstruction such as DIOS [34,85]. Even though this manifestation can be diagnosed and treated successfully with a water-soluble enema or air enema, the recurrence rate is high [34].

Therefore, the evidence indicates that reduced intestinal motility in CF patients may contribute to MI, DIOS, constipation, and abdominal pain that will affect the quality of life of these patients.

1.2.2.7 GI dysmotility in CF

A variety of theories have been purposed to explain the anomalies in CF patients' guts. The distal ileum and colon are the most critical locations affected by CF dysfunction compared to the esophagus and the stomach[92]. Much of the research on GI complications in CF patients have concentrated on epithelial and fluid transport abnormalities[19,93]. CFTR on the apical membrane of the intestine works with other transporters such as the Epithelial Sodium Channel (ENaC) and a sodium proton exchanger, to regulate luminal fluidity and pH [94]. The amount of CFTR messenger RNA (mRNA) is the highest in the duodenum and progressively decreases to the ileum. There is also a high level of CFTR mRNA in the mucus-secreting Brunner's gland [87,94]. Areas with high levels of CFTR mRNA indicate an increased need for bicarbonate and fluid secretion. Dysfunctional CFTR channels decrease bicarbonate transport in the gut and result in the dehydrated intestinal lumen, decreased fluid secretions, and postprandial acidity[87]. The altered luminal environment gives rise to the accumulation of mucus and the predisposition of other diseases such as intestinal obstruction, dysbiosis, and inflammation[25]. These can contribute to the intestinal dysmotility in CF patients.

In addition, dysbiosis is a distortion of the gut biota and has also been proposed to contribute to GI abnormalities displayed by patients. One of the most common manifestations in CF patients is small intestine bacterial overgrowth (SIBO). In a healthy individual, the overall number of bacteria in the intestine is smaller compared to that of the large intestine. Mechanisms like peristalsis, migrating motor complex, antibacterial protein, and intestinal fluid maintain the bacterial count low[87]. However, in CF patients, the accumulation of thickened mucus provides an anchor for bacteria overgrowth. Like a vicious cycle, increased bacterial load stimulate more mucus production, which leads to mucus and bacterial plug[87]. The large intestine microbiota can also alter due to altered intestinal milieu or frequent use of antibiotics. These factors may disturb the symbiotic relationship between the intestinal microbiota and the GI tract[87]. This symbiotic relationship is affected when the composition of the microbiota changed in CF patients. CF

children have increased *E.coli* compared to others[95]. *Ruminococcus gnavus* is found in CF patients but not in healthy individuals. Some have suggested that since *R. gnavus* is a mucin degrader, and preferentially selected[87,96].

Small intestine bacterial overgrowth can cause inflammation and disrupt gut motility[92]. With CF patients experiencing various intestinal complications such as mucosal edema, erythema, ulceration, there can be intestinal injuries that lead to inflammation of the gut. There are also findings suggesting inflammatory-associated gene upregulation and enterocytes damages[87]. The inflammation could derive from chronic NSAIDs use in patients. Other than smooth muscle dysfunction, CF-related intestinal dysmotility can derive from SIBO or an increase of prostaglandin due to inflammation[87].

Other than the effect of CFTR mutation on the GI epithelia, there is evidence of malfunctioning of the nervous system and muscle[97]. CFTR is also found in the central and peripheral nervous system, especially the myenteric ganglia of the ENS. Thus, CFTR dysfunction may result in the lack of stimulation of gut motility[92]. Unfortunately, little is known about the effect of CFTR mutation on GI tract contractility due to neuron or muscle cell malfunction. Research has shown that CF dysfunction can downregulate choline acetyltransferase in the colon, which would decrease the formation of acetylcholine[98]. In terms of transit time in CF patients, others have purposed a delay in the overall passage of chyme through the small intestine for CF patients[99]. In this study, we test the contractility characteristics of the small intestine of swine models of cystic fibrosis.

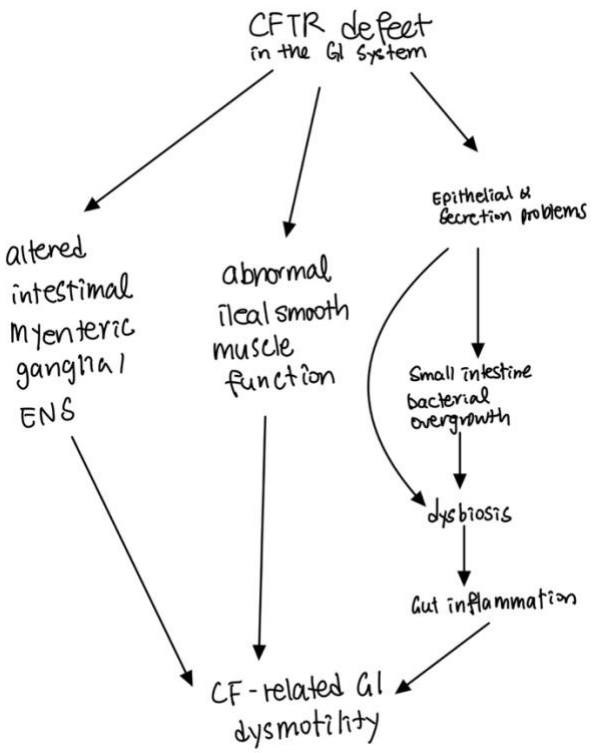

Figure 1-7: Different theories purposed to explain CF-related gastrointestinal dysmotility[92].

1.3 Rationale of study

CF had previously been considered a pediatric disease due to the short life expectancy experienced/suffered by the patients [6,7]. With extensive research and the discovery of various treatments, the average life expectancy of CF patients has steadily increased over the last six decades, and luckily CF is no longer just a pediatric disease, and currently, more than 50% of CF patients are adults in US and Canada [34]. As CF patients live into adulthood, there has been a greater interest in studying CF complications that had been previously overlooked in favor of life-threatening lung disease research. One such complication is gastrointestinal malfunctions that lead to GI tract constipation or blockage, abdominal discomfort, and pain [34].

The contribution of abnormal muscle contraction to GI complications has not been studied in-depth. There is a lack of understanding on the contribution of abnormal contractility of the GI tract smooth muscle to reduced chime transit and predisposition to obstruction suffered by CF patients. Therefore, we decided to use a swine model of cystic fibrosis (CFTR knockout, $CFTR^{-/-}$) to compare the differences between the CF and the wild-type intestine. Swine models

were used because they are one of the best models for CF experiments and its CFTR amino acid sequence is 92% identical with the human protein[1]. We used an isolated organ bath system to compare the CF and wild-type ileum contractions. We choose to use the ileum of the small intestine because the most serious CF-related intestinal obstruction complications tend to occur in the ileum and proximal large intestine [87].

1.4 Hypothesis and objectives

1.4.1 Hypothesis

Mutations in the CFTR gene affect the smooth muscle contraction in the GI tract. Thus, we hypothesize that $CFTR^{-/-}$ pig ileum would have reduced peristaltic contractions compared to wild-type pig ileum.

1.4.2 Objectives

The objective of this experiment is to compare the gastrointestinal motility between wild-type and CF pig ileum. We used both newborn (day 0 after birth) and one-week-old pigs (day 5 to 7 after birth). For CF pigs, we used CFTR gene knocked out ($CFTR^{-/-}$) pigs from the Exemplar Genetics (Iowa, USA). We used an isolated organ bath system to quantify ileum contraction. We studied their basal peristalsis and their contraction in response to three important neurotransmitters in the GI system, acetylcholine, serotonin, and histamine. To explore potential receptor differences between wild-type and CF tissues, we induced contraction by the neurotransmitters in the presence of increasing concentrations of the neurotransmitters' corresponding antagonists (atropine, methysergide, and cetirizine).

CHAPTER 2. MATERIALS AND METHODS

2.1 Animals

All experiments were performed with the approval of the Animal Ethics Committee and all the University of Saskatchewan guidelines were followed.
Animal Utilization Protocol Number: 2011047
Biosafety Permit: PHS-15

2.1.1 Animal models

There are different animal models used for cystic fibrosis research [100]. The five most commonly used are pigs, ferrets, rabbits, rats, and mice [100]. Mice were the first animal model developed for CF research, with the first CFTR knockout mouse model developed as early as 1992, just three years after the discovery of the CFTR gene [1,101]. Mice models are appropriate for CF-related intestinal disease but mice do not develop spontaneous lung, pancreatic, and hepatic-related diseases [1,31,100]. The fact that CFTR knockout mice do no develop CF disease led to the search for other models that better replicate the human CF condition. In mid-2008, both ferrets and pig models were developed. The swine model was shown to best replicate the respiratory, pancreatic, and hepatic-related CF diseases [1,31,83]. More recently, rat and rabbit models were developed. However, there is little literature on these models, and hard to determine how well these animals replicate human CF disease [100].

$CFTR^{-/-}$ Porcine models

We decided to use pigs for our research as they are one of the best animal models for CF research. We used wild-type (WT) and CFTR knockout ($CFTR^{-/-}$) pigs at day 0 after birth (newborn) and day 5-7 after birth (one-week-old).

The first CF pigs were developed by *Welsh et al.* using adeno-associated virus vectors to target the *cftr* gene in the fibroblast cells in the fetal pigs [102]. These cells are then used as nuclear donors for somatic cell nuclear transfer into oocytes to generate heterozygous male pigs. Through heterozygous breeding, they were able to produce $CFTR^{-/-}$ pigs [103,104]. They found that $CFTR^{-/-}$ pigs develop spontaneous lung disease that closely resembles the human CF condition

[102,103]. Moreover, CFTR$^{-/-}$ swine developed meconium ileus with a 100% incidence, as well as pancreatic destruction [102,103].

Another advantage of using pigs is that the anatomy of the pig GI system is very similar to the human digestive system, and it has the general structure found in all domestic animals. The small intestine of a pig is also divided into duodenum, jejunum, and ileum [105]. Similar to the human body, the function of the small intestine is also in charge of digestion and absorption in the pig, except digestion in pigs can also occur through fermentation. For this experiment, we decided to use the ileum to test our hypothesis.

CFTR$^{-/-}$ swine were purchased from Exemplar Genetics (Iowa, USA). These animals were gut-corrected, as they have restored CFTR function at the *epithelium* of the gastrointestinal (GI) tract, which improves the survival of the CF piglets since they do not develop meconium ileus but does not restore CFTR in muscle or nerve cells. Since the CFTR function was not restored in either the smooth muscle of neurons, it doesn't affect the result of our experiment on GI motility.

To produce gut-corrected CFTR$^{-/-}$ swine cloned embryos carrying the gut correction construct (TgFABP>pCFTR pigs) are produced and implanted in a surrogate wild-type. The sow was then transported from Iowa to the University of Saskatchewan and housed in quarantine for four weeks at the Western College of Veterinary Medicine Animal Care Unit, University of Saskatchewan. Cesarean section was performed to deliver the piglets to minimize the stress in the birth canal [106]. There were seven pigs delivered in total. Veterinary specialists monitored the health of the animals 24h a day by recording feeding, heart rate, ventilation rate, temperature, activity, urination, and defecation. The piglets were hand-fed with bovine colostrum replacer and medicated as necessary. A university veterinarian monitored the health of the animals, and if a preestablished humane endpoint was reached the animal was then euthanized. The animals were imaged at the Canadian Light Source for an unrelated project. Then, the animals were euthanized by exsanguination, and tissues of interest were dissected, including the GI tract for this project. Experimentation started within 15 minutes after euthanasia and lasted several hours. Out of the seven piglets, four were euthanized within 24h after birth (newborn group), and two were euthanized on day 5 and day 7 (one-week-old group).

The wild-type swine were purchased from Prairie Swine Centre, University of Saskatchewan, Canada. The wild-type pigs were euthanized using captive blot. In total, we had 9 wild-type neonate pigs and 15 wild-type postnatal one-week-old pigs [107].

2.1.2 Tissue Dissection

The animal carcass was disinfected with 70% ethanol and placed in a holder in a supine position. We dissected the carcass; the cecum was identified first to help us to find the location of the ileum. The GI tract was clamped with a hemostat at the end of the ileum before the cecum. A second hemostat was then clamped 10 cm apart from the first hemostat on the ileum. Both ends of the ileum were then removed and placed in ice-cold Tyrode's solution (137 mM NaCl, 2.7 mM KCl, 1.8 mM $CaCl_2$, 0.121 mM $MgCl_2$, 11.9 mM $NaHCO_3$, 0.04 mM NaH_2PO_4, 5.55 mM Glucose) aerated with carbogen (95% O_2 + 5% CO_2 mixture) until the tissue was mounted on the experimental apparatus.

For mounting tissues onto the organ bath systems, two Petri dishes, two tweezers, one syringe, a surgical needle, and surgical thread were needed. Cold oxygenated Tyrode's solution was first poured into the two Petri dishes. A 1-2 cm section of the ileum tissue was transferred into one of the two Petri dishes. We then used a syringe to clean the content of the ileum two times. Finally, we used a surgical needle and thread to make an attachment to the experimental apparats on both ends of the preparation (*Figure 2-1*). The ileum section was then transferred and mounted to the organ bath system.

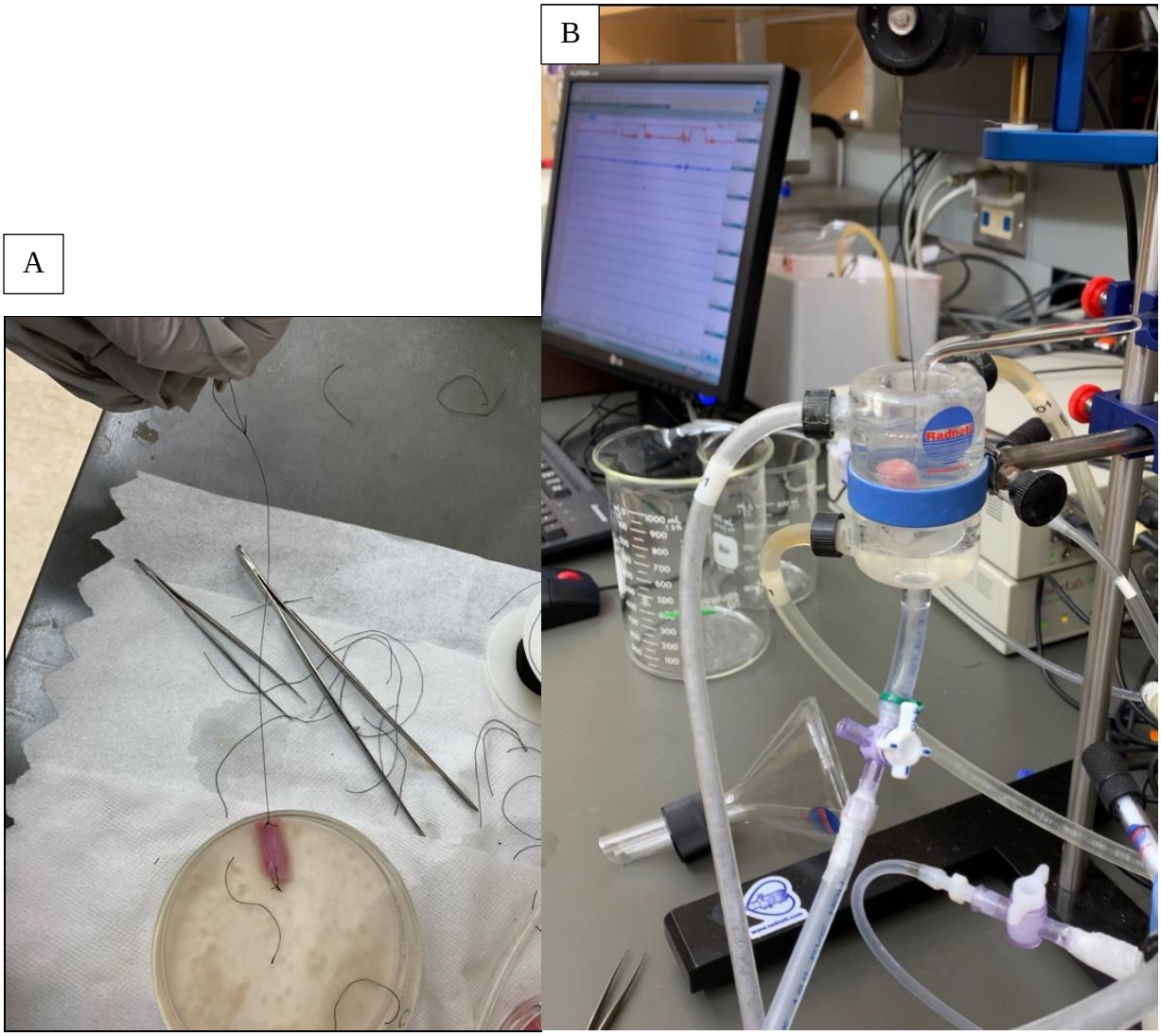

Figure 2-1: The process of mounting a section of the pig ileum on to the isolated organ bath system. A) The process of inserting string to the ileum section in preparation for mounting. B) A picture of a section of the pig ileum mounted to the isolated organ bath.

2.2 Isolated organ bath system

We used a multi-chamber isolated organ bath system to record the motility of the GI tract *in vitro*. The ileum preparation was mounted in an organ bath chamber (10ml) and aerated with 95% O_2- 5% CO_2 and maintained at 37 °C. The tissue was connected through a thread loop to an isometric force transducer to measure the change in force produced by contraction or relaxation of the tissue. The signal produced by the force transducer was amplified by an amplifier and

digitized by a data acquisition system (PowerLab) connected to a computer. The data were analyzed using the software LabChart.

Two tubes were connected to each organ bath and they were fitted with three-way stopcock valves. One tube allows Tyrode's solution from a reservoir to go down to each individual organ bath while the other tube empties the solutions in the organ bath. Thus, by opening and closing these valves, we were able to drain the content of the chamber and wash out substances added to the organ bath, after recording responses. A third glass tube was connected to the organ bath to allow continuous aeration (with 95% O_2 – 5% CO_2) of the tissues.

The organ bath system was calibrated before experimentation. To calibrate, a weight of 2g was hanged on the tension adjuster, and the signal produced by the force transducer was set as 2g. Then the weight was removed, and the new recording was calibrated as 0g.

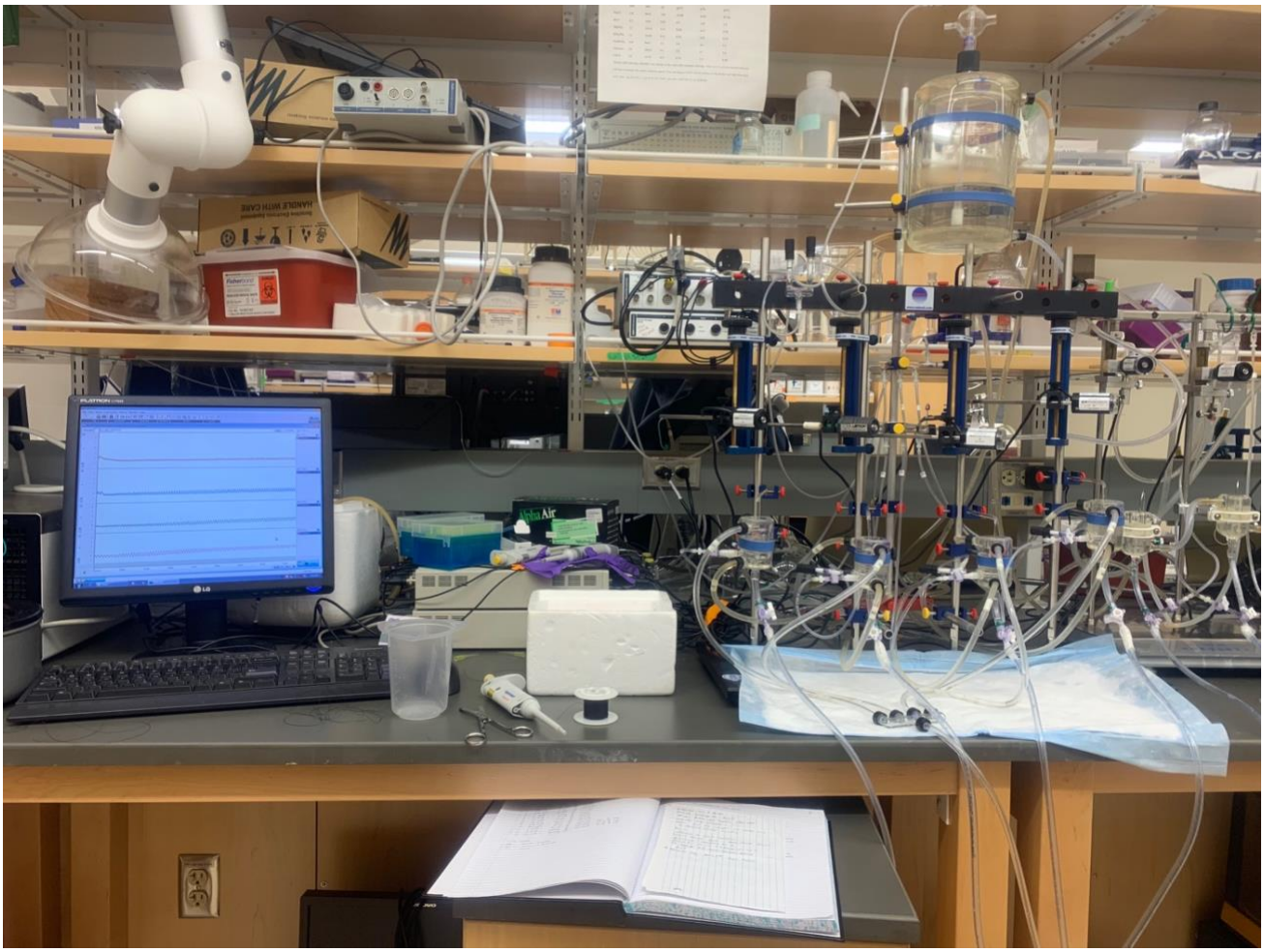

Figure 2-2: A picture of the isolated organ bath apparatus used for the experiment that is located in the lab of the health sciences building of the University of Saskatchewan.

2.3 Data collection

2.3.1 Experimental protocol

After mounting the ileum tissues on the organ bath system, a 1g tension was applied to the tissue in 0.2g increments until the force transducer recorded a constant 1g. Then the tissue was left to acclimatize, until the preparation presented of constant peristaltic waves. The experiment consisted of first measuring spontaneous motility, followed by exposing the preparations to increasing concentrations of neurotransmitters, and lastly repeat the process after incubating in different concentrations of neurotransmitter receptor antagonists (*Table 2-1* and *Figure 2-3*).

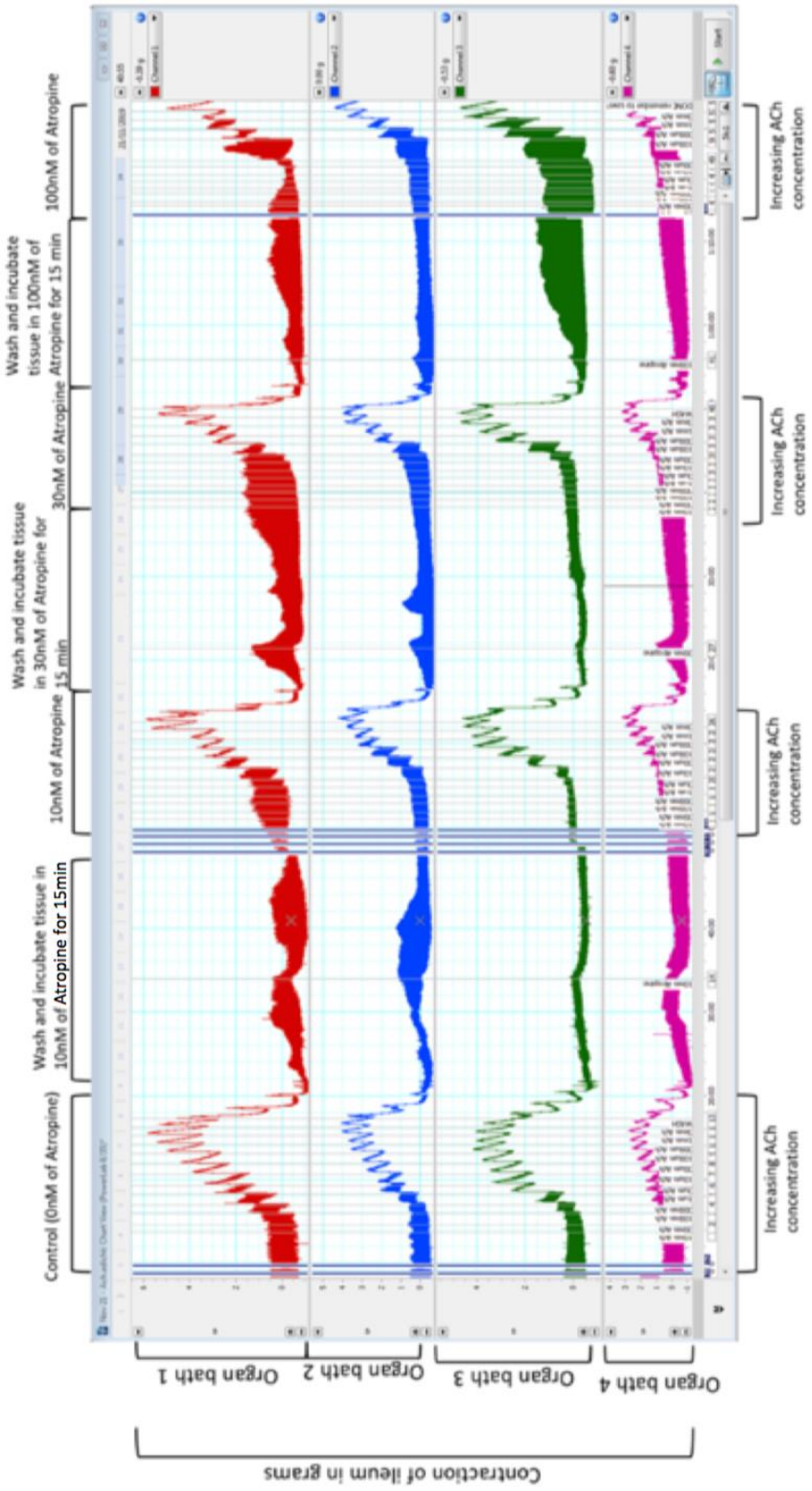

Figure 2-3: A screenshot of the raw data using LabChart software.

We tested the agonists at 10nM, 30nM, 100nM, 300nM, 1 µM, 3 µM, 10 µM, 30 µM, 100 µM, 300 µM, 1mM, and 3mM. After a set of experiments was finished, the organ bath was washed three times by first emptying the organ bath solution and then adding fresh solution. Then, we tested the effect of the antagonist by incubating the tissue with the antagonist at three different concentrations for 15 minutes before testing the effect of the neurotransmitter.

Table 2-1: The different concentrations of antagonists used in the experiment.

Atropine (Acetylcholine antagonist)	**Methysergide** (Serotonin antagonist)	**Cetirizine** (Histamine antagonist)
0 nM	0 µM	0 µM
10 nM	1 µM	1 µM
30 nM	3 µM	3 µM
100 nM		

2.3.2 Measured parameters

We measured the contraction tension (in grams) at each neurotransmitter concentration induced by the neurotransmitter (*Figure 2-4,* see black arrows), then we identified the maximum contraction tension for each contraction (*Figure 2-4,* see red-circled black arrow). We also measured the contraction force amplitude and frequency. To measure peristaltic movement frequency, we counted the number of waves and divided them by the time (in seconds). To find the amplitude, we used the same section of peristalsis recording and found the average of all the amplitudes of each wave selected (*Figure 2-5*). We used gram as the unit of the amplitude measurement because we calculated the amplitude as the difference between the maximum point of the wave (in g) minus the minimum point of the wave (in g).

Finally, to compare the effect of neurotransmitter receptor blockers, we normalized contraction tension (percent maximal contraction tension) at each neurotransmitter concentration to the maximum tension produced by each preparation and plotted the data as a concentration (dose)-response curve (see below). The percent maximal response is calculated by taking the contraction tension at a specific concentration of agonist and divided by the maximum contraction tension and multiply by 100.

$$Percent\ maximum\ contraction = \frac{Contraction\ at\ a\ concentration\ in\ grams}{Maxium\ contraction\ in\ grams} \times 100\%$$

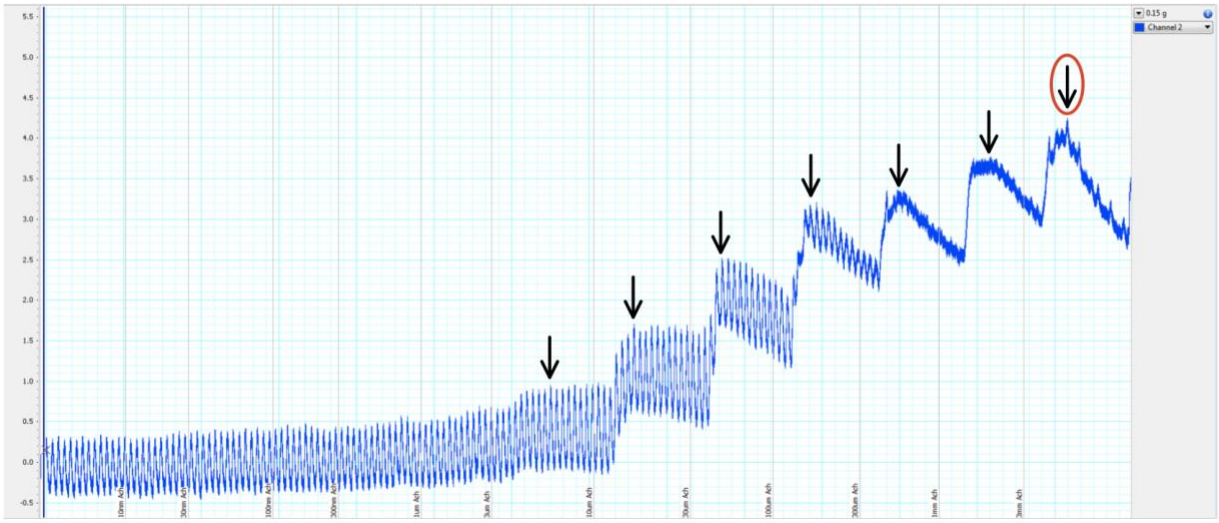

Figure 2-4: A sample trace of an experiment that shows the point to choose for each concentration (arrow pointing) and the maximum concentration for the set of experiment (circled in red).

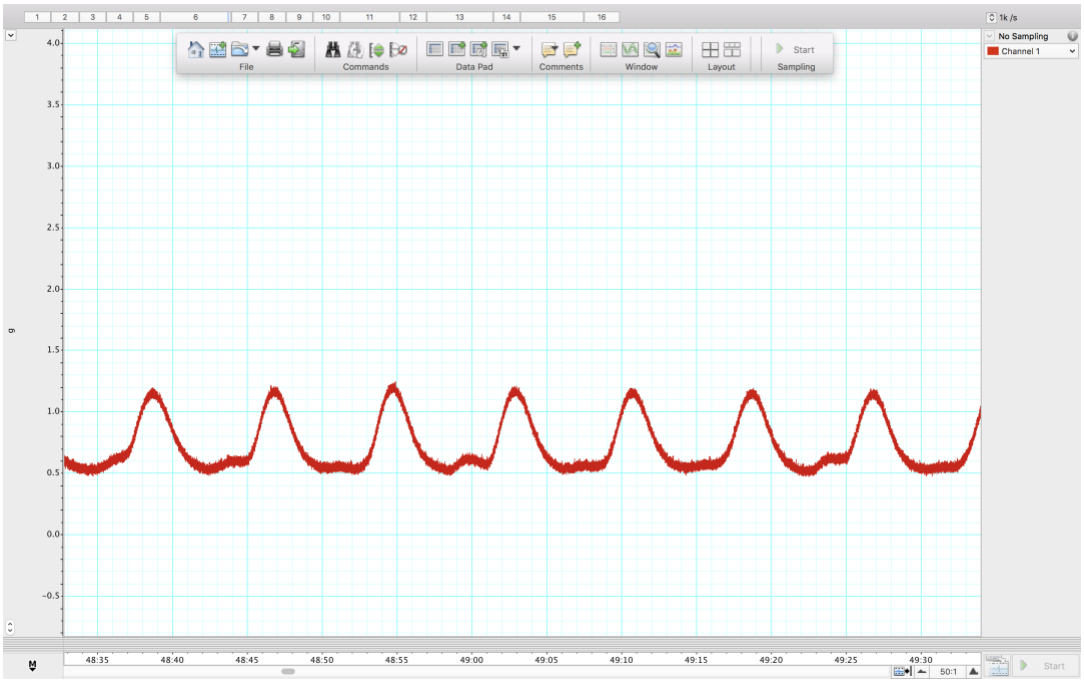

Figure 2-5: A sample trace of a section of pig ileum peristalsis.

2.4 Data statistics and plotting

We used Graphpad Prism 9 to analyze all the data and producing the figures. We then used the One-way ANOVA test/Two-way ANOVA test (since we have 4 different groups) to find out if there were significant differences present between the groups. A P value less than 0.05 was taken as significant. We used One-way ANOVA test to compare basal peristalsis, maximum contraction tension, and amplitude and frequency. To compare contraction tension, we used Two-way ANOVA test (Dunnett's multiple comparison test). Lastly, to compare dose-response curves in each group, we used Extra sum-of-squares F test.

Dose-response curve

The x-axis of a dose-response curve represents concentrations (or logarithmic of the concentration), and the y-axis represents the percent contraction tension. Some important parameters can be calculated from the dose-response curves. EC_{50} is the concentration that produces a half-maximal response. E_{max} represents the maximum contraction tension. The agonist dose-response curve shifts to the right in the presence of antagonists (*Figure 2-6*).

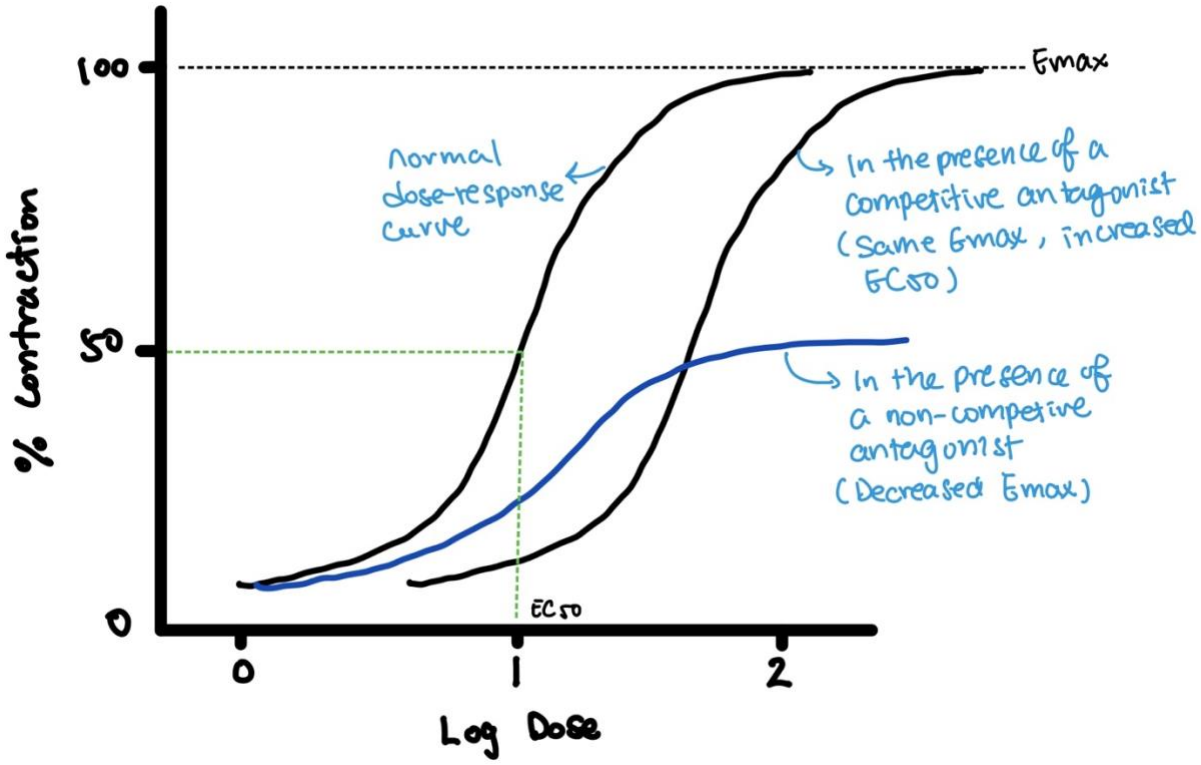

Figure 2-6: Example of dose-response graphs with EC_{50}, and Emax labeled and changes due different types of antagonists. Modified from [108].

Schild plot

The Schild plot, created by Heinz Otto Schild in 1959, is a tool for analyzing the effect of agonists and antagonists on receptor response [109]. To plot a Schild plot, one needs at least three EC_{50} values of the agonist in the presence of three different concentrations of the same antagonist. The x-axis of the plot is the negative log of the concentration of the antagonist, and the y-axis is the log of dose-ratio (DR) minus one. DR can be calculated using the EC_{50} of an agonist in the presence of an antagonist divided by the EC_{50} of an agonist in the absence of an antagonist [110].

$$Dose\ Ratio\ (DR) = \frac{EC_{50} of\ an\ agonist\ in\ the\ presence\ of\ an\ antagonist}{EC_{50}\ in\ the\ absence\ of\ antagonist\ (control)}$$

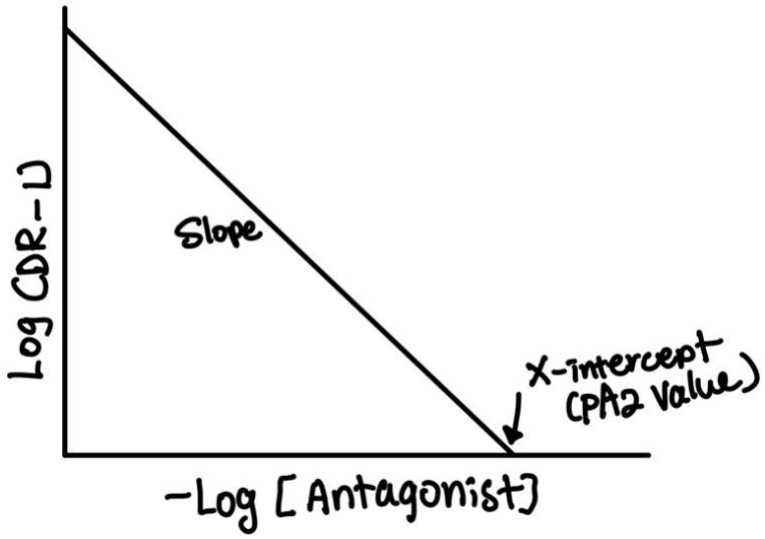

Figure 2-7: An example of a Schild pot showing the pA_2 value. Modified from [111].

One of the important values obtained from the Schild plot is the pA_2 (or pA_x) value, which indicates antagonist affinity. The pA_2 value is the concentration of antagonist when double the agonist is required to have the same effect as when no antagonist is present [110]. The X-intercept of a Schild plot is the pA_2 value, the negative logarithm of the molar concentration of the antagonist needed to double the concentration of the agonist to elicit the same response obtained in the absence of antagonist [110,112]. Furthermore, the same receptor expressed in different tissues will have the same pA_2 values. It is helpful to identify the presence of identical receptors in different tissues, when the same of agonist and antagonist are used [110]. Schild plot is also helpful in determining the type of antagonism of a drug on the receptor. For instance, a competitive antagonist will exhibit a straight line with a slope of -1 on the Schild plot and -log K_B=pA_2 value for a dose-ratio of x=2 [109]. Other types of antagonism would have a slope different from -1.

CHAPTER 3. RESULTS

3.1 Basal ileum peristalsis

We observed that there were constant peristaltic waves after mounting the ileal tissues on the isolated organ bath system. We decided to measure the peristaltic contraction amplitude and frequency in order to compare the cystic fibrosis (CF) and wild-type (WT) swine phenotypes before any treatment. There was a significant difference in the amplitude of peristaltic waves, with the wild-type ileum displaying a statistically significant larger amplitude of peristalsis compared to $CFTR^{-/-}$ ileum tissues (*Figure 3-2A*). However, there is no significant difference in the frequency of peristalsis (*Figure 3-2B*). The average amplitude of wild-type newborn (WTp0) tissue was 0.81 ± 0.11 g (*n*= 36), $CFTR^{-/-}$ newborn (CFp0) was 0.35 ± 0.06 g (*n*=32), wild-type one-week-old (WTp7) was 0.93 ± 0.10 g (*n*=59), and $CFTR^{-/-}$ one-week-old (CFp7) was 0.35 ± 0.10 g (*n*=16). The data shows that wild-type tissue peristaltic amplitude is almost three times larger than that of CF tissues.

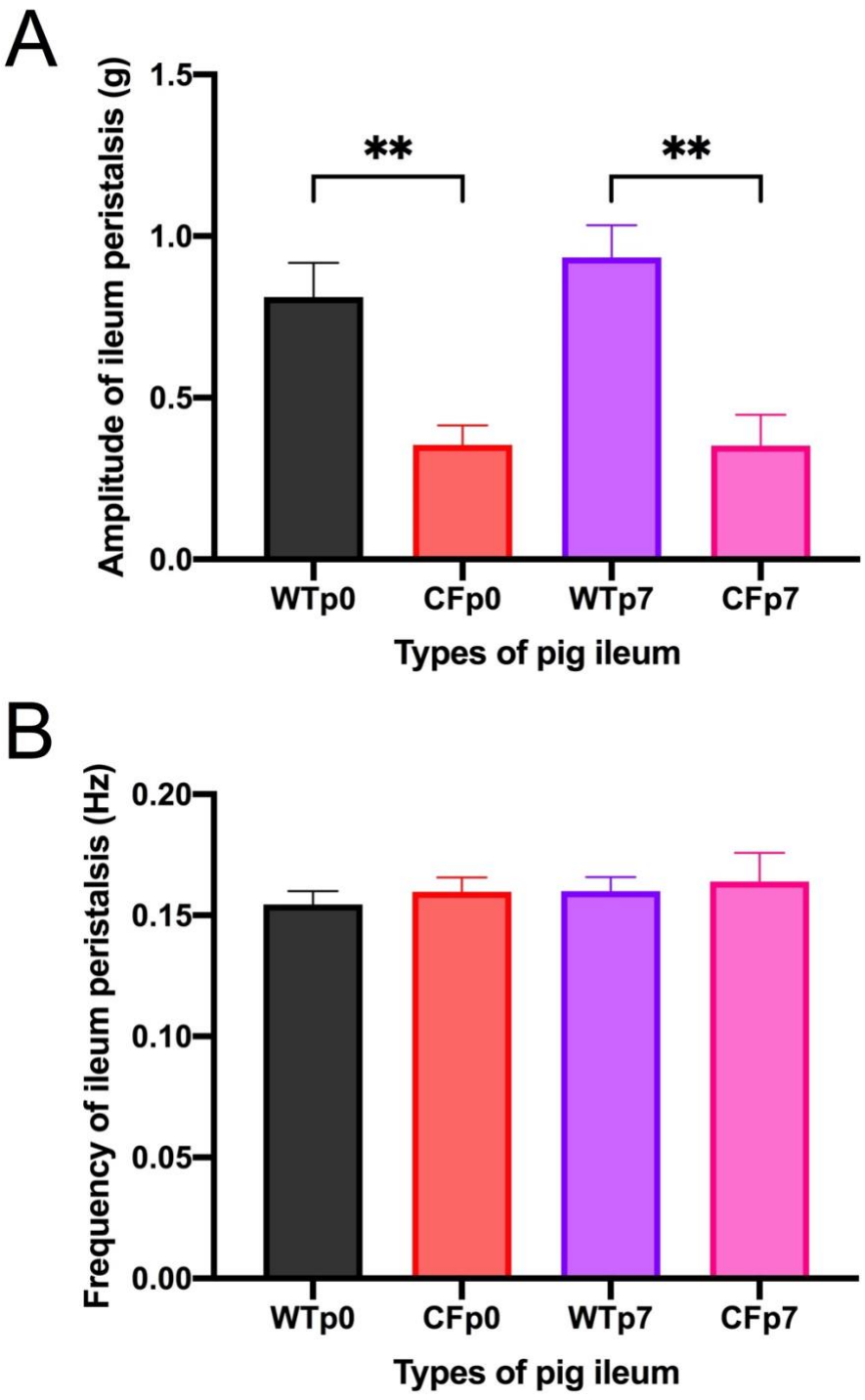

Figure 3-1: Average basal amplitude and frequency of ileum peristaltic waves in wild-type neonate (WTp0), CFTR$^{-/-}$ neonate (CFp0), wild-type one-week-old (WTp7), CFTR$^{-/-}$ one-week-old (CFp7) swine (WTp0, n= 36 assays from 9 pigs; CFp0, n= 32 assays from 4 animals; WTp7 n= 59 assays from 15 animals; CFp7, n= 16 assays from 4 animals). Data is presented as mean

*± SEM. A) Average amplitude of basal ileum peristalsis grams (g) of WTp0, CFp0, WTp7 and CFp7. (One-Way ANOVA test, Tukey's multiple comparisons test, ** = P < 0.01; *** = P < 0.001). B) Average frequency of basal ileum peristalsis in Hertz (Hz) of WTp0, CFp0, WTp7 and CFp7. Average amplitude of WTp0 = 0.15 ± 0.01 Hz, CFp0=0.16 ± 0.01Hz, WTp7= 0.16 ± 0.01 Hz, CFp7 = 0.16 ± 0.01 Hz (no significant differences, One-Way ANOVA test).*

3.2 Ileum contraction in response to acetylcholine

3.2.1 Contraction tension and maximum contraction tension

All the experimental groups responded to ACh with a significant increase in contraction tension compared to the baseline (*Figure 3-2*). Furthermore, neonate wild-type tissue responded with a lower effective bath concentration of ACh, at around 300 nM (-6.5 log M), and 1 µM (-6 log M) for CF tissues (*Figure 3-2*). Wild-type one-week-old tissue also responded at a lower concentration of ACh, with a significant increase in tension at 10 nM (-8 log M), and 1 µM (-6 log M) for CF preparations (*Figure 3-2*). However, we found that there is no significant difference of contraction tension between the CF and wildtype responses at either age group *(WTp0, n= 17 assays from 9 pigs; CFp0, n= 16 assays from 4 animals; WTp7 n= 29 assays from 11 animals; CFp7, n= 8 assays from 2 animals; Two-way ANOVA test, Dunnett's multiple comparison test).*

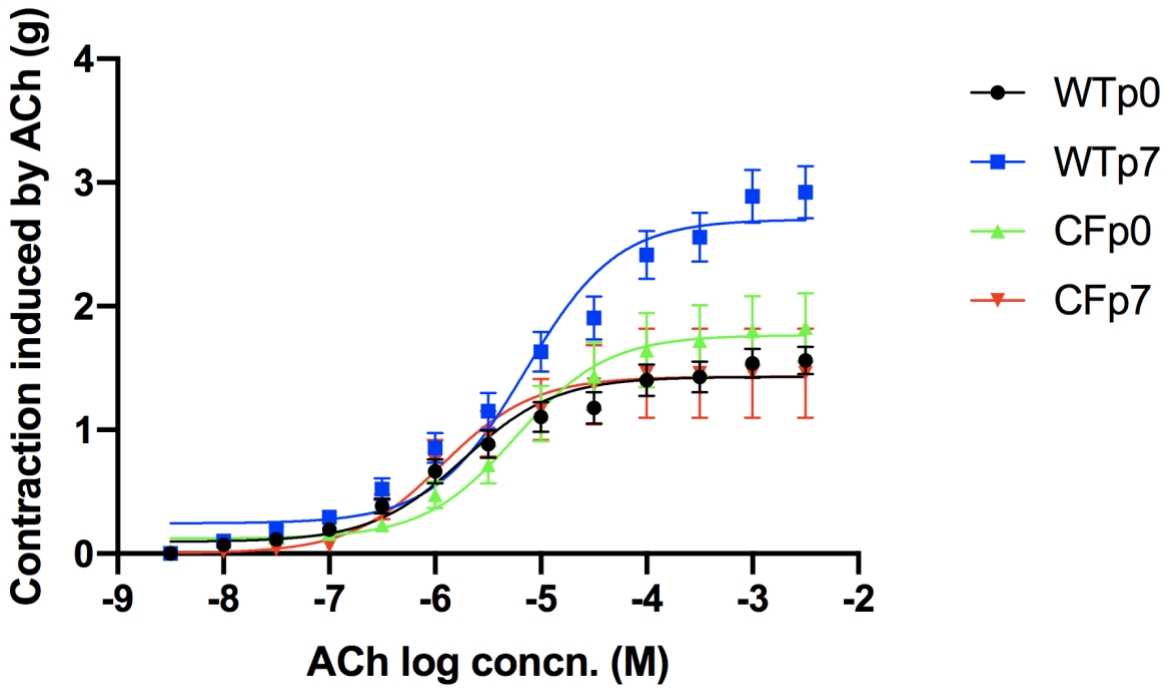

Figure 3-2: Contraction tension fitted through a dose-response curve induced by ACh in wild-type neonate (WTp0), CFTR$^{-/-}$ neonate (CFp0), wild-type one-week-old (WTp7), CFTR$^{-/-}$ one-week-old (CFp7) swine (WTp0, n= 17 assays from 9 pigs; CFp0, n= 16 assays from 4 animals; WTp7 n= 29 assays from 11 animals; CFp7, n= 8 assays from 2 animals). Data is presented as mean ± SEM.

To further test the response of ACh, we analyzed the maximum contraction tension displayed by tissue preparations during all sets of experiments in *Figure 3-3*. The results show that the capability for maximum contraction tension by wild-type one-week-old ileum was significantly larger than wild-type neonates and CFTR$^{-/-}$ one-week-old. There was no difference between wild-type and CFTR$^{-/-}$ neonates. The wild-type one-week-old pig ileum had a maximum ileum contraction of 2.94 ± 0.18 g (n=29), and wild-type neonate pig ileum had a maximum ileum contraction of 1.56 ± 0.11 g (n=17). CFTR$^{-/-}$ neonate pig ileum had a maximum ileum contraction of 1.84 ± 0.27 g (n=16) and CFTR$^{-/-}$ one-week-old was 1.46 ± 0.36 g (n=8). The maximum ileum contraction of wild-type one-week-old was approximately two times larger compared to the other types of tissues.

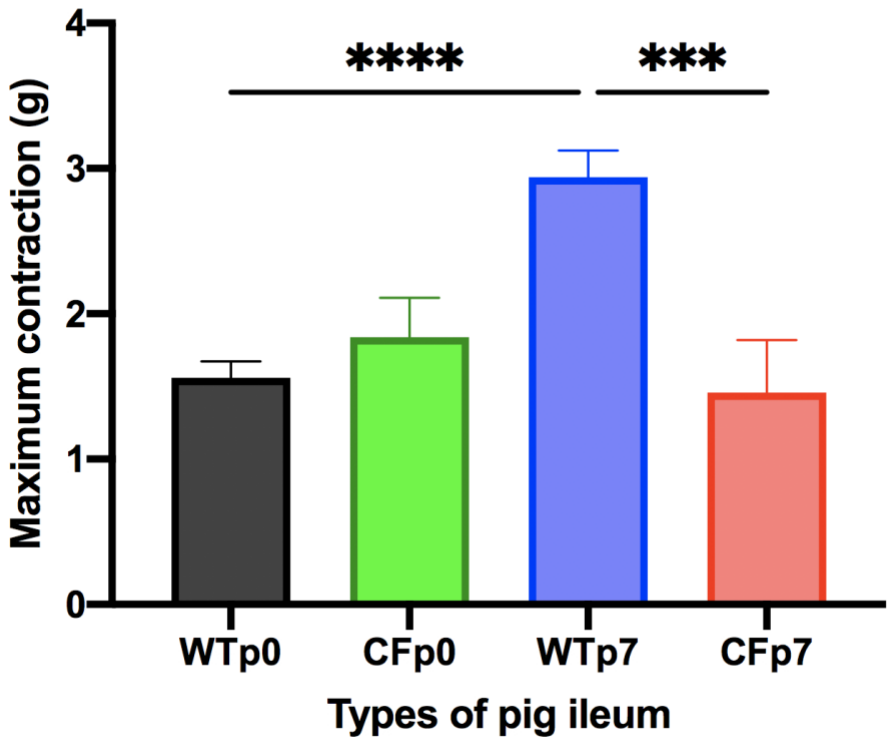

*Figure 3-3: ACh-induced maximum contraction in wild-type neonate (WTp0), CFTR$^{-/-}$ neonate (CFp0), wild-type one-week-old (WTp7), CFTR$^{-/-}$ one-week-old (CFp7) swine (WTp0, n= 17 assays from 9 pigs; CFp0, n= 16 assays from 4 animals; WTp7 n= 29 assays from 11 animals; CFp7, n= 8 assays from 2 animals). Data is presented as mean ± SEM (One-Way ANOVA test, Tukey's multiple comparisons test, ** = P < 0.01; *** = P < 0.001; **** = P < 0.0001).*

3.2.2 Amplitude and Frequency post ACh stimulation

We were also interested in looking at the amplitude and frequency of contraction after neurotransmitter stimulation. The amplitude and frequency were obtained at each increasing concentration of ACh (*Figure 3-4*). We see that the amplitude of both wild-type tissues decreased significantly with an increasing concentration of ACh stimulation. Wild-type neonate pig ileum started to have a significant decrease in amplitude from baseline at 10 µM (-5 log M) of ACh and wild-type one-week-old pig ileum started to have a significant decrease at 3 µM (-5.5 log M) of ACh. The decrease of peristaltic contraction may be associated with an increase in

muscle tone. However, there were no significant differences observed in the CFTR$^{-/-}$ pigs (*Figure 3-5*). We conclude that there were no differences in the frequency of peristaltic waves.

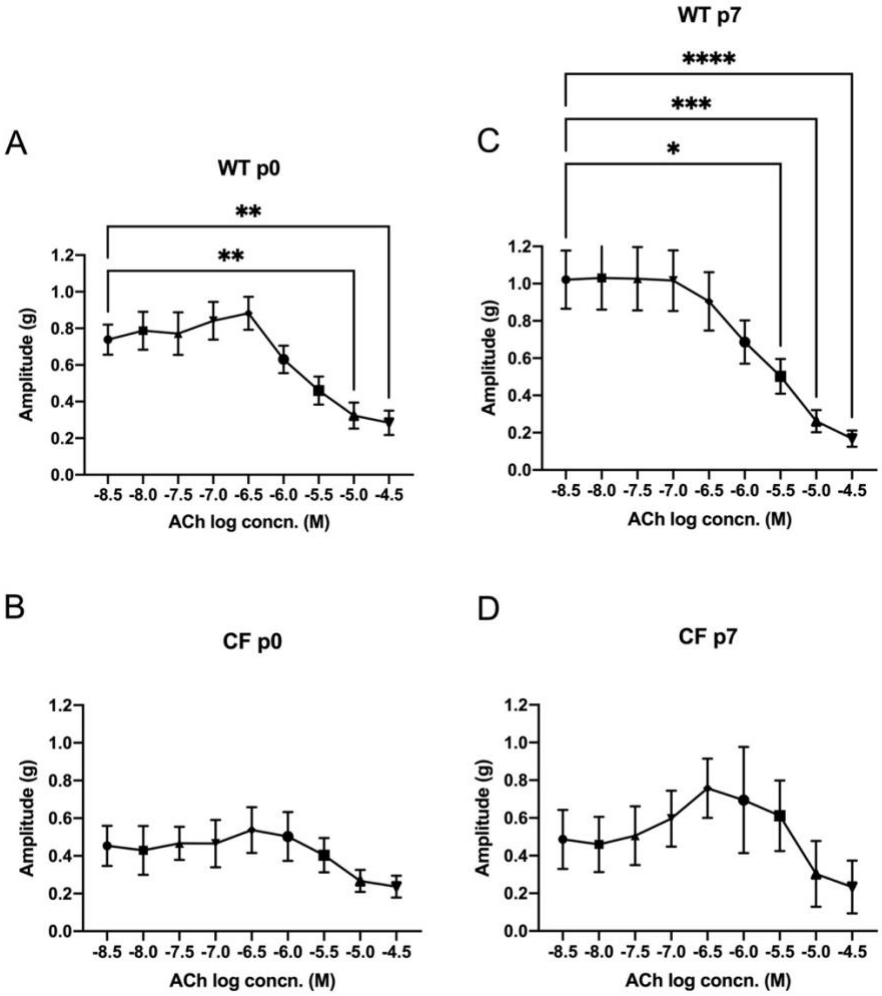

*Figure 3-4: Amplitude of peristaltic waves with increasing concentration of ACh in wild-type neonate (WTp0), CFTR$^{-/-}$ neonate (CFp0), wild-type one-week-old (WTp7), CFTR$^{-/-}$ one-week-old (CFp7) swine (WTp0, n= 17 assays from 9 pigs; CFp0, n= 16 assays from 4 animals; WTp7 n= 29 assays from 11 animals; CFp7, n= 8 assays from 2 animals). A-D) Amplitude of peristaltic waves. There was a significant decrease in amplitude from the baseline amplitude at 10 µM (-5 log M) and 3 µM (-5.5 log M) for WTp0 and WTp7 tissues, respectively. One-Way ANOVA, Dunnett's multiple comparison test was conducted to compare each point with the baseline first datapoint, ** = P < 0.01; *** = P < 0.001; **** = P < 0.0001. Data is presented as mean ± SEM.*

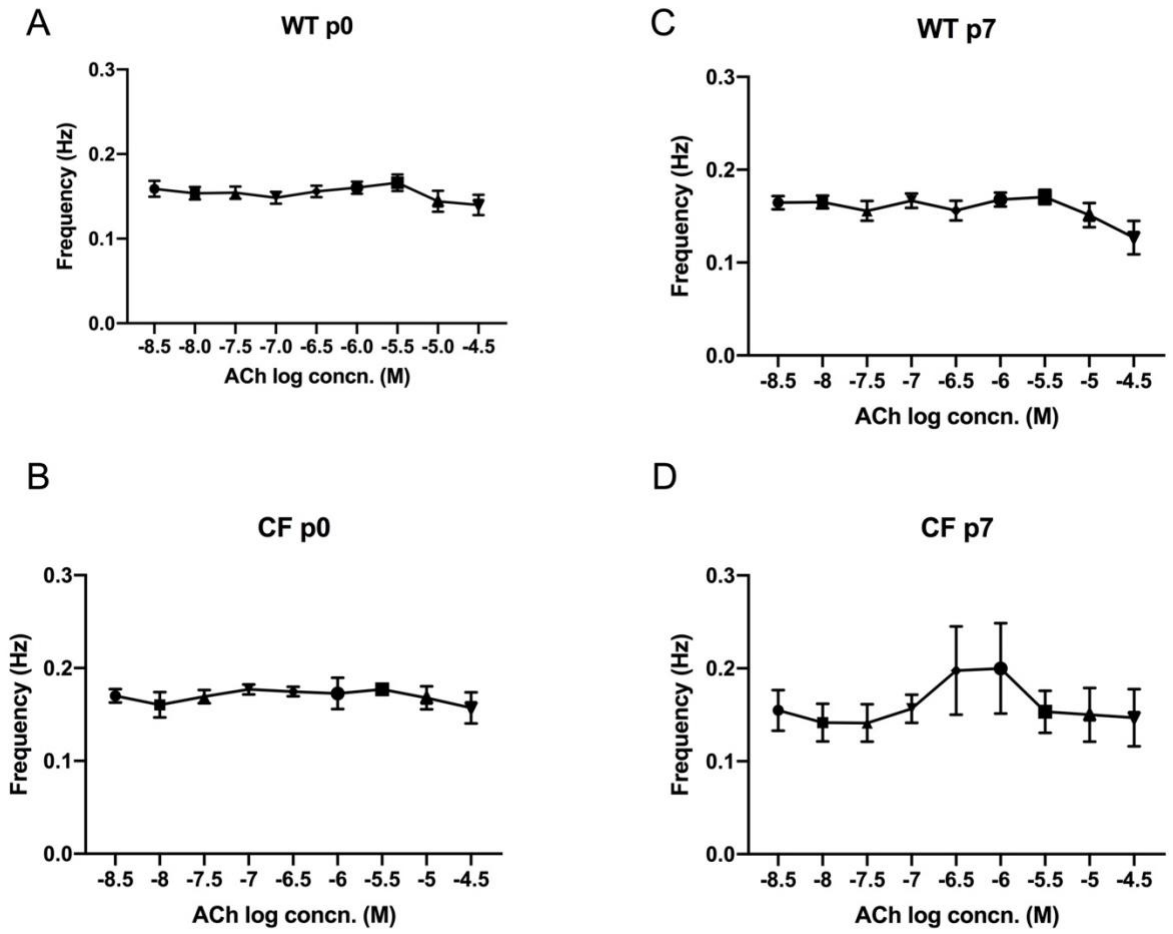

Figure 3-5: Frequency of peristaltic waves with increasing concentration of ACh in wild-type neonate (WTp0), CFTR$^{-/-}$ neonate (CFp0), wild-type one-week-old (WTp7), CFTR$^{-/-}$ one-week-old (CFp7) swine (WTp0, n= 17 assays from 9 pigs; CFp0, n= 16 assays from 4 animals; WTp7 n= 29 assays from 11 animals; CFp7, n= 8 assays from 2 animals). A-D) Frequency of peristaltic waves. There is no significant difference between each point and its baseline frequency (One-Way ANOVA). Data is presented as mean ± SEM.

3.2.3 Effect of atropine on ACh dose-response curve

We decided to compare the response of the receptor in response to the ACh in the absence and presence of its antagonist, atropine, by producing a normalized ACh dose-response curve after treatment with three different concentrations of antagonist atropine and using the values obtained to graph a Schild plot, which provides the information about the affinity of the antagonist to the receptor. Since the contractility of the preparation depends on the phenotype,

we decided to normalize the response to the maximum contraction tension to make it possible to compare between CF and WT preparations. The dose-response curves were obtained by plotting the percent of maximum contraction tension in response to each concentration of ACh. For each graph in the curves fitting that data are statistically different from each other (*Figure 3-6*, Extra sum-of-squares F test).

All tissues demonstrate competitive antagonism of atropine with ACh, represented as the curves move to the right and reach the same maximal response. All the EC_{50} values for each type of tissue increase with increasing concentration of atropine (*Table 3-1*). However, even though all the curves are statically different from each other for each type of tissue, we didn't find a significant difference between the EC_{50} values.

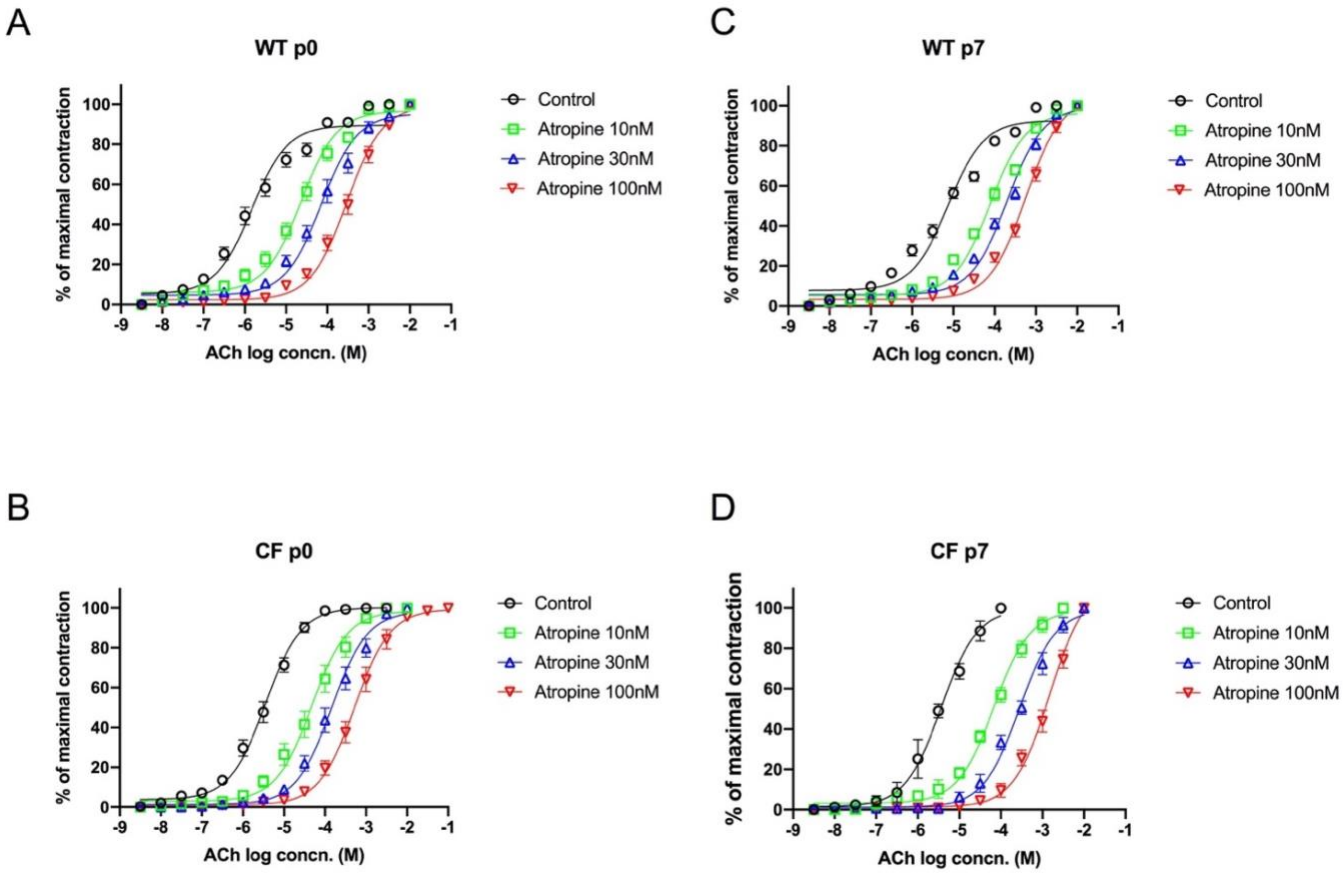

Figure 3-6: Dose-response curve of ACh-induced contraction in the presence of 3 different concentrations of antagonist atropine in wild-type neonate (WTp0), CFTR$^{-/-}$ neonate (CFp0), wild-type one-week-old (WTp7), CFTR$^{-/-}$ one-week-old (CFp7) swine (WTp0, n= 17 assays from 9 pigs; CFp0, n= 16 assays from 4 animals; WTp7 n= 29 assays from 11 animals; CFp7, n= 8 assays from 2 animals). Dose-response curve of ACh-induced contraction on A) WTp0 pigs, B) CFp0 pigs, C) WTp7 pigs, and D) CFp7 pigs. The curves are significantly different (Extra sum-of-squares F test). Data is presented as mean ± SEM.

Table 3-1: EC_{50} values of ACh-induced contraction with increasing concentrations of atropine.

	ACh alone (μM)	ACh +atropine 10nM (μM)	ACh +atropine 30nM (μM)	ACh +atropine 100nM (μM)
Wild-type neonates	1.47	23.1	71.6	293.7
$CFTR^{-/-}$ neonates	3.56	47.3	144.4	525.4
Wild-type one-week-olds	7.42	78.3	201.6	556.3
$CFTR^{-/-}$ one-week-olds	3.65	68.3	279.9	1494

3.2.4 Schild plot

We used the EC_{50} values from the dose-response curve (*Table 3-1*) to produce the Schild plot. The x-axis of the plot is the negative log concentration of the antagonist atropine, while the y-axis is the log dose-ratio minus one. The x-intercept of the graph is also the pA_2 value that indicates the affinity of the antagonist to the receptor. The slope of the plot also gives information about the type of antagonism on the receptor, usually, a slope close to -1 indicates competitive antagonism [109]. A slope different from -1 can indicate non-competitive antagonism or competitive antagonism involves different receptor subtypes [113].

For neonate pigs (day 0), we found that the pA_2 values for wild-type and CF are 9.017 and 9.003, respectively (*Figure 3-7*). For one-week-old pigs, we found that the pA_2 values for wild-type and CF are 9.099 and 8.904, respectively. For the slope of the Schild plot, neonate wild-type and CF are -1.131 and -1.076, respectively. For one-week-old wild-type and CF tissue, the slopes are -0.8893 and -1.363, respectively. The slopes for neonate tissues are not different from each other, and since both values are very close to -1, it reaffirms that atropine is a competitive antagonist. The slope for one-week-old tissues, however, are significantly different from each other and not very close to -1. It suggests that the tissue might express more than one receptor subtype, with different responses to the competitive antagonist atropine.

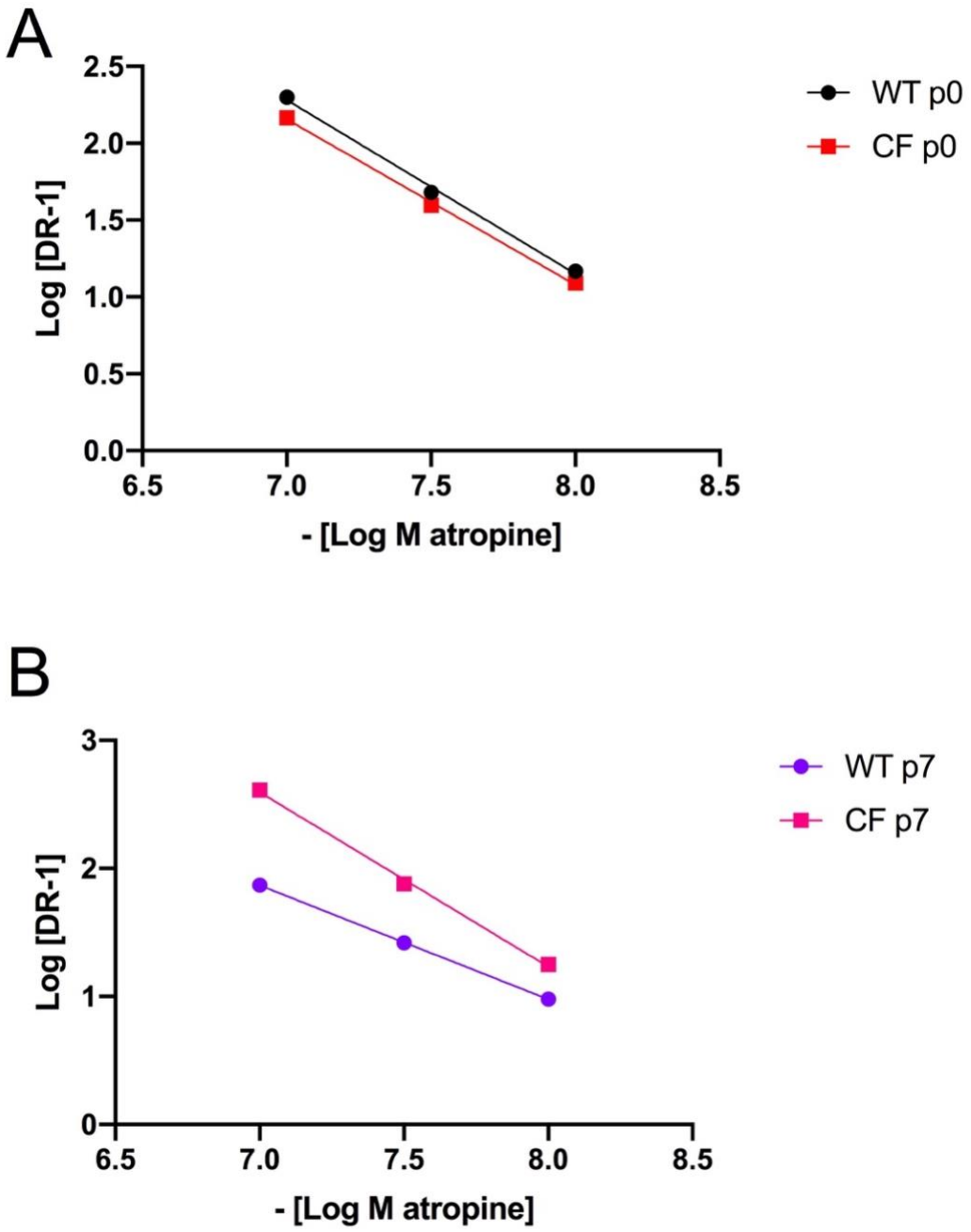

Figure 3-7: Schild plot of ACh-induced contraction in A) neonate preparations and B) one-week-old preparations. (WTp0, n= 17 assays from 9 pigs; CFp0, n= 16 assays from 4 animals; WTp7 n= 29 assays from 11 animals; CFp7, n= 8 assays from 2 animals).

Table 3-2: The slopes, intercepts, equations and R square values of the Schild plots.

	Slope	Y-intercept	X-intercept (pA_2 value)	Equation	R square
Wild-type neonates	-1.131	10.2	9.017	$y = -1.131x + 10.20$	0.9969
$CFTR^{-/-}$ neonates	-1.076	9.691	9.003	$y = -1.076x + 9.691$	0.9989
Wild-type one-week-olds	-0.8893	8.092	9.099	$y = -0.8893x + 8.092$	0.9999
$CFTR^{-/-}$ one-week-olds	-1.363	12.13	8.904	$y = -1.363x + 12.13$	0.9982

3.3 Ileum contraction in response to serotonin

The tissues did not respond very well to serotonin compared to ACh. Thus, we decided to count how many, of the total number of experiments, reacted to serotonin and the two different concentrations of antagonist methysergide (*Table 3-3*). If the tissue had consistent peristalsis, we included it in our analysis. If the tissue had consistent peristalsis but does not have any increase in contraction in response to serotonin, we categorize that tissue as not reacting to the neurotransmitter. We also tested some unresponsive tissues with a high concentration of ACh as a positive control for the viability of the tissue and those preparations responded as expected to ACh.

Table 3-3 The number of tissues that had noticeable reaction to serotonin.

	Serotonin alone	Serotonin + methysergide 1µM	Serotonin + methysergide 3µM
Wild-type neonates	8/9	8/9	8/9
$CFTR^{-/-}$ neonates	8/8	6/8	2/8
Wild-type one-week-olds	13/13	12/13	12/13
$CFTR^{-/-}$ one-week-olds	4/4	4/4	2/4

(The denominator is the total number of experiments conducted and the numerator is the number of tissues that reacted to serotonin.)

3.3.1 Contraction tension and maximum contraction tension

With all the tissues that have some reaction to serotonin, we analyzed their contraction tension (g) in response to serotonin (*Figure 3-8*). For neonate tissues, wild-type responded to serotonin-induced contraction at 300 nM (-6.5 log M), while CF tissue started to respond at 100 nM (-7 log M). CF neonate tissue reached the maximum at 300 nM (-6.5 log M) but stopped having a significant contraction after 3 µM (-5.5 log M). For one-week-old tissues, wild-type tissue had a significant response starting from 30 nM (-7.5 log M), while CF tissue did not have a significant response. However, there was no difference between wild-type and CF at either age.

We then obtained the maximum contraction tension induced by serotonin (*Figure 3-9*). We found that the maximum contraction tension was 0.61 ± 0.07 g (n=8) for wild-type neonate, 0.62g ± 0.15 g (n=8) for CF neonate, 0.90g ± 0.12 g (n=13) for wild-type one-week-old, and 0.99g ± 0.32 g (n=4) for CF one-week-old. However, we did not find any significant differences between each group.

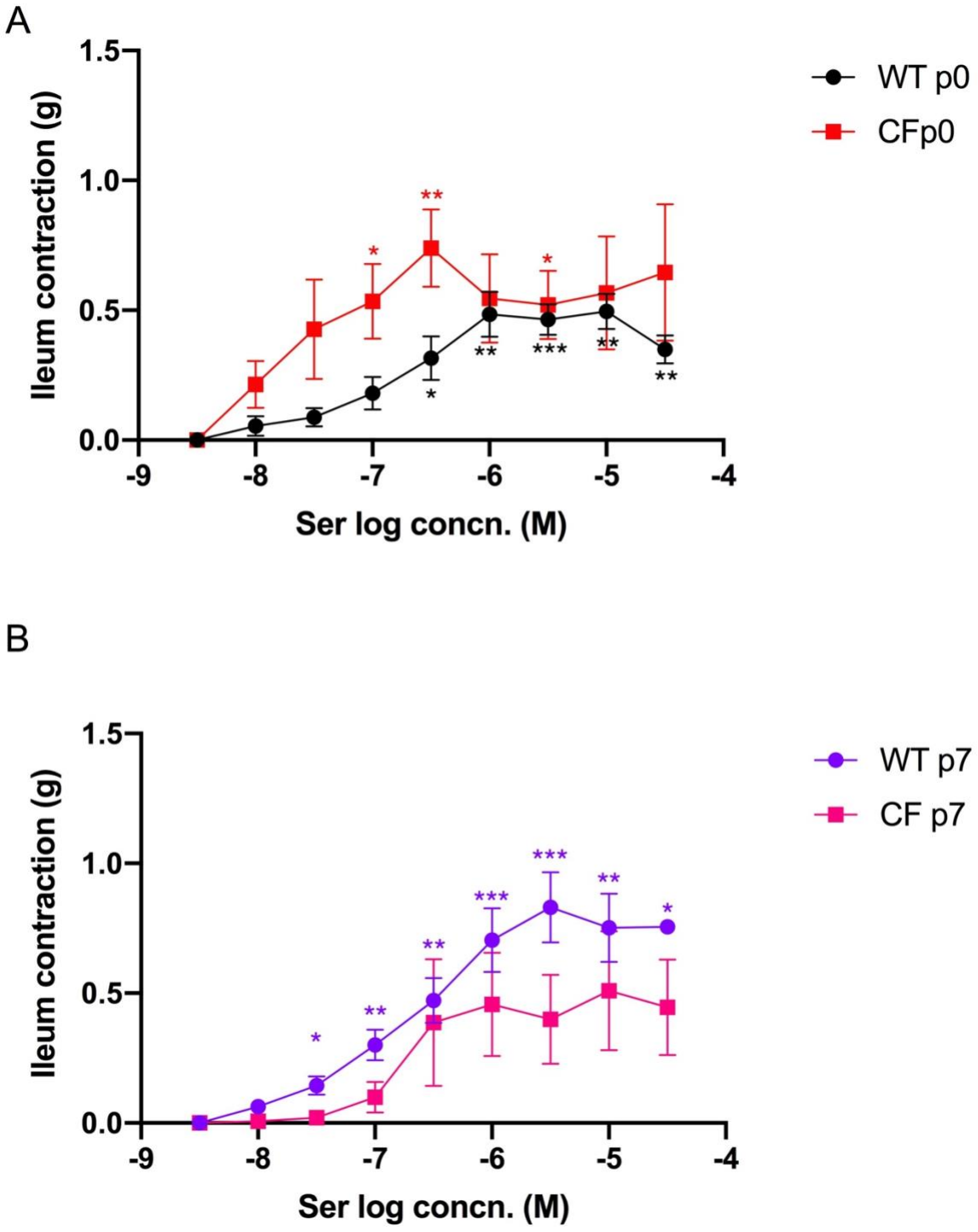

Figure 3-8: Contraction tension induced by serotonin in wild-type neonate (WTp0), CFTR$^{-/-}$ neonate (CFp0), wild-type one-week-old (WTp7), CFTR$^{-/-}$ one-week-old (CFp7) swine (WTp0, n= 8 assays from 8 pigs; CFp0, n= 8 assays from 4 animals; WTp7 n= 13 assays from 9 animals; CFp7, n= 4 assays from 2 animals). A) Average contraction induced by serotonin in

*neonate pigs. B) Average contraction induced by serotonin in one-week-old pigs (Two-way ANOVA, Dunnett's multiple comparison test was conducted to compare each point with the baseline first data point. * = P <0.05; ** = p < 0.01; *** = p < 0.001; **** = p < 0.0001). Data is presented as mean ± SEM.*

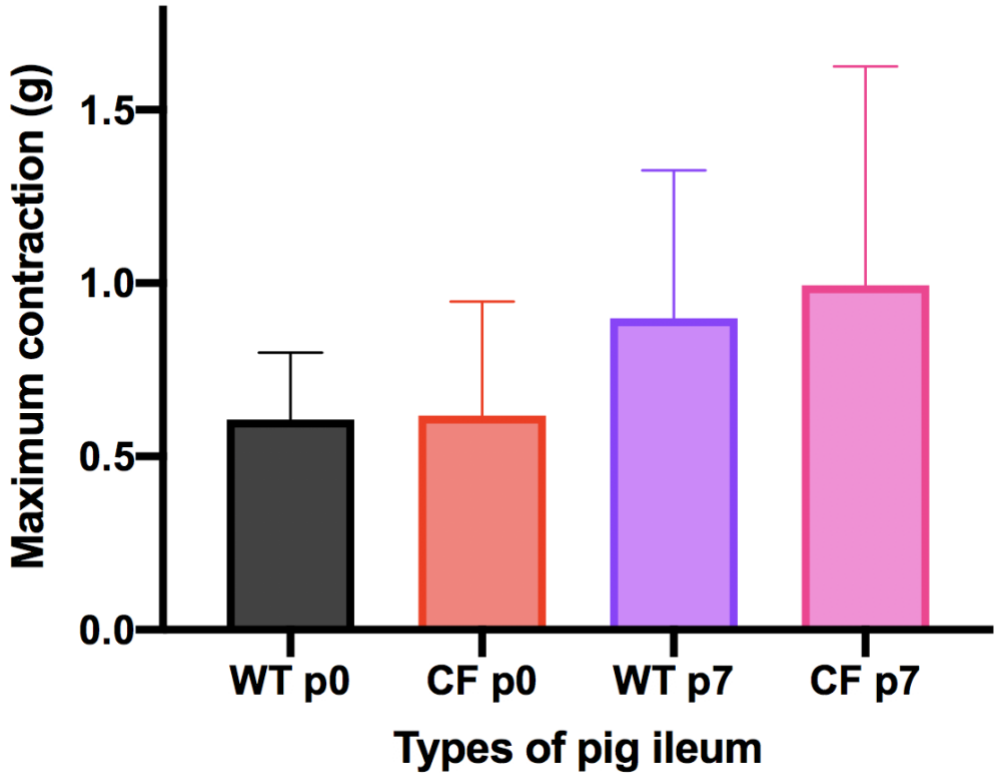

Figure 3-9: The maximum contraction tension induced by serotonin in wild-type neonate (WTp0), CFTR$^{-/-}$ neonate (CFp0), wild-type one-week-old (WTp7), CFTR$^{-/-}$ one-week-old (CFp7) swine (WTp0, n= 8 assays from 8 pigs; CFp0, n= 8 assays from 4 animals; WTp7 n= 13 assays from 9 animals; CFp7, n= 4 assays from 2 animals, One-way ANOVA test). Data is presented as mean ± SEM.

3.3.2 Amplitude and Frequency post serotonin stimulation

Since there were only two sets of data for the amplitude of the CFTR one-week-olds available to analyze, we decided to separate them to point form instead of line form (*Figure 3-10D*). We didn't see any significant differences in the amplitude and frequency of peristaltic waves post increasing concentration of serotonin. Since there was not enough CF data collected for serotonin, the error bars were quite big. Furthermore, with fewer data collected, it is less likely to find significance.

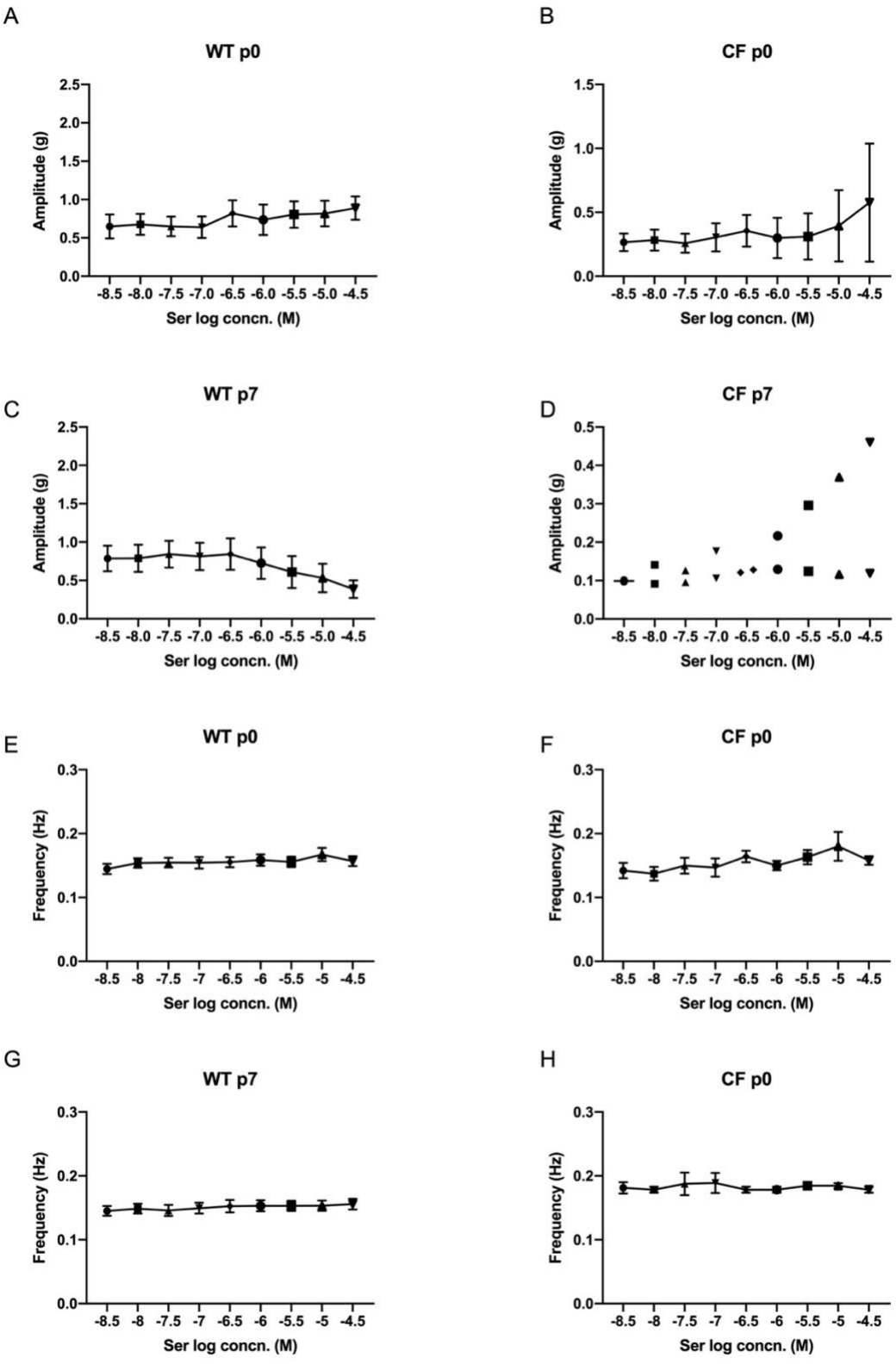

Figure 3-10: Amplitude and frequency of peristaltic waves with increasing concentration of serotonin in wild-type neonate (WTp0), CFTR$^{-/-}$ neonate (CFp0), wild-type one-week-old

(WTp7), CFTR$^{-/-}$ one-week-old (CFp7) swine (WTp0, n= 8 assays from 8 pigs; CFp0, n= 8 assays from 4 animals; WTp7 n= 13 assays from 9 animals; CFp7, n= 2 assays from 2 animals). A-D) amplitude of peristaltic waves in response to serotonin for wild-type p0, CFp0, wild-type p7, and CFp7, respectively. There is no significant difference (One-Way ANOVA) between each point and the baseline first point. D) Since there were only 2 sets of data that had consistent peristaltic waves for CF one-week-old tissue, the data was then plotted into a two-point form on the graph. E-H) Frequency of peristaltic waves in response to serotonin for wild-type p0, CFp0, wild-type p7, and CFp7, respectively. There is no significant difference between each point and the baseline (first point, One-Way ANOVA). Data is presented as mean ± SEM.

3.3.3 Effect of methysergide on serotonin dose-response curve

The dose-response curves were plotted for all four different types of tissues in response to serotonin. We could see that the wild-type tissues follow the expected trend that is with increasing concentration of the antagonist, the dose-response curve shifts to the right (*Figure 3-11 A and C*). However, the CFTR$^{-/-}$ tissues responded very poorly and did not adhere to what we were expecting. There could be two reasons that we obtained these unexpected results. First, we did not have enough CF data and were thus less likely to find a very cohesive conclusion with the limited data we had. Secondly, *Figure 3-8* shows that CF tissues respond very poorly to serotonin. Since the tissues already respond very poorly to serotonin, thus the effect of the antagonist is less evident. The EC_{50} values of the different types of tissues in different concentrations of methysergide are listed in *Table 3-4*.

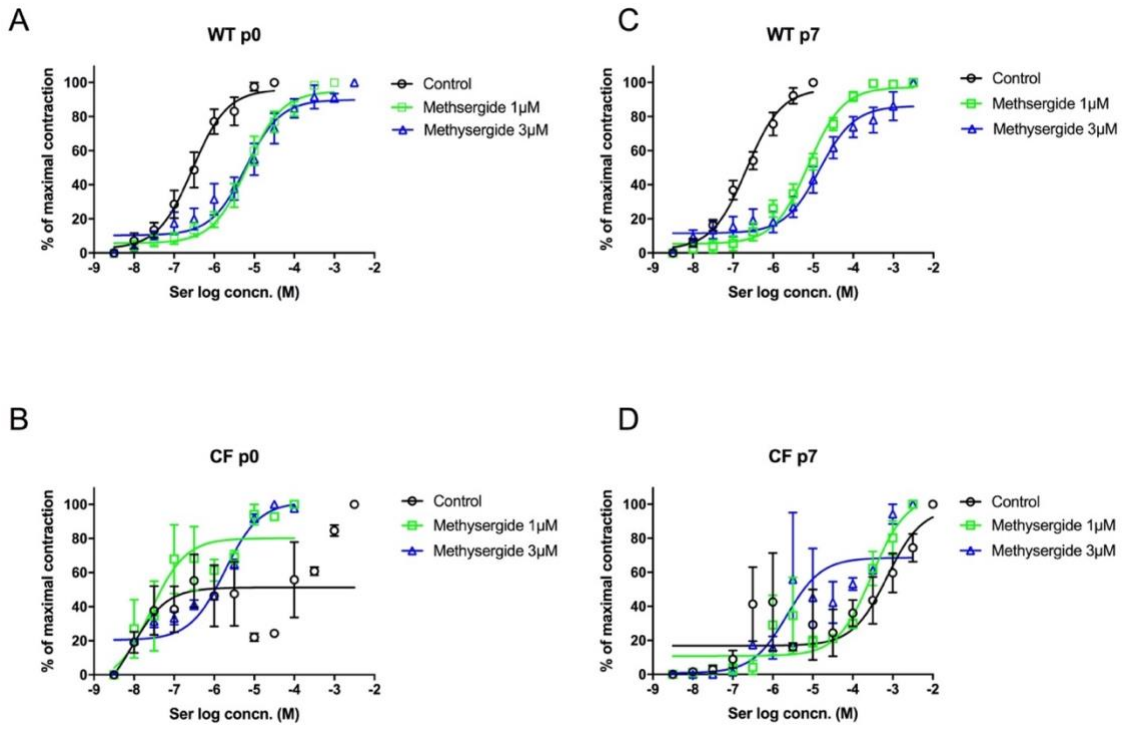

Figure 3-11: Dose-response curve of wild-type and swine ileum tissues induced by serotonin (Ser) in the presence of two different concentrations of antagonist methysergide in wild-type neonate (WTp0), CFTR$^{-/-}$ neonate (CFp0), wild-type one-week-old (WTp7), CFTR$^{-/-}$ one-week-old (CFp7) swine (WTp0, n= 8 assays from 8 pigs; CFp0, n= 8 assays from 4 animals; WTp7 n= 13 assays from 9 animals; CFp7, n= 2 assays from 2 animals). A-D) Dose-response curve of wild-type p0, CFp0, wild-type p7, and CFp7, respectively. For each graph from A-D, the curves are significantly different (Extra sum-of-squares F test). Data is presented as mean ± SEM.

Table 3-4: EC_{50} values of serotonin-induced contraction with increasing concentrations of methysergide.

	Serotonin alone (µM)	Serotonin + methysergide 1µM (µM)	Serotonin + methysergide 3µM (µM)
Wild-type neonates	0.288	6.66	6.13
CFTR$^{-/-}$ neonates	0.00890	0.0263	1.84
Wild-type one-week-olds	0.217	7.5	14.5
CFTR$^{-/-}$ one-week-olds	725	299	2.25

3.4 Ileum contraction in response to histamine

The last neurotransmitter we decided to test was histamine since it plays an important role in the GI tract. However, the tissues did not respond well to this neurotransmitter. It could be that histamine plays more of a modulatory role in the response of other neurotransmitters such as ACh (*Table 3-5*). Tissue preparations were considered viable if they displayed consistent peristalsis after mounting on the isolated organ bath. The tissue reaction to histamine was worse with increasing concentration of the antagonist cetirizine. Furthermore, neonate wild-type tissue did not respond well to histamine (*Table 3-5*).

Table 3-5 The number of tissues that had noticeable reaction to histamine.

	Control	Histamine + Cetirizine 1µM	Histamine + Cetirizine 3µM
Wild-type neonates	5/9	4/9	3/9
$CFTR^{-/-}$ neonates	8/8	8/8	2/8
Wild-type one-week-olds	17/17	13/17	10/17
$CFTR^{-/-}$ one-week-olds	3/4	3/4	2/4

(The denominator is the total number of experiments conducted and the numerator is the number of tissues that reacted to histamine.)

3.4.1 Contraction tension and maximum contraction

There was a significant increase in contraction compared to the baseline for wild-type tissues, while the increase in CF tissues was not significant (*Figure 3-12 A and B*). Both CF tissues have a higher ileum contraction than wild-type but are not significantly different from the baseline. This is most likely due to the small sample size of the CF tissues. Significance can be potentially obtained by increasing the sample size of CF tissues.

We then analyzed the maximum contraction tension induced by histamine (*Figure 3-13*). We found that the average maximum contraction for wild-type neonate was 0.87 ± 0.13 g (n=5), CF neonate was 1.16 ± 0.24 g (n=8), wild-type one-week-old was 1.38 ± 0.20 g (n=17) and CF one-week-old was 1.92 ± 0.42 (n=3). However, we didn't see any significant differences between each group of tissues.

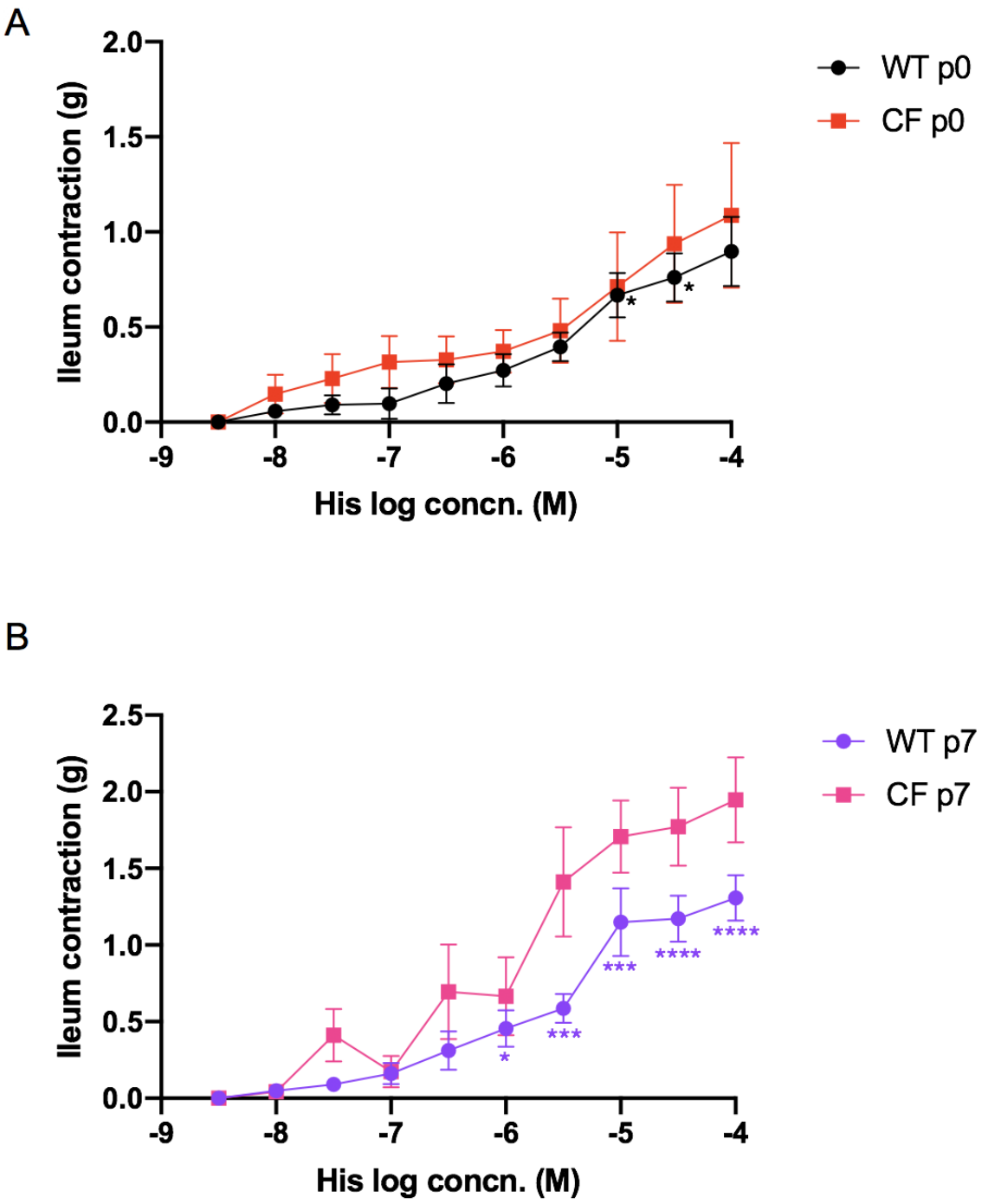

Figure 3-12: Contraction tension induced by histamine in wild-type neonate (WTp0), CFTR$^{-/-}$ neonate (CFp0), wild-type one-week-old (WTp7), CFTR$^{-/-}$ one-week-old (CFp7) swine (WTp0, n= 5 assays from 8 pigs; CFp0, n= 8 assays from 4 animals; WTp7 n= 17 assays from 11

*animals; CFp7, n= 3 assays from 2 animals). A) Average contraction induced by histamine on neonate pigs. B) Average contraction induced by histamine in one-week-old pigs (Two-way ANOVA, Dunnett's multiple comparison test was conducted to compare each point with the baseline first data point. * = P <0.05; ** = p < 0.01; *** = p < 0.001; **** = p < 0.0001). Data is presented as mean ± SEM.*

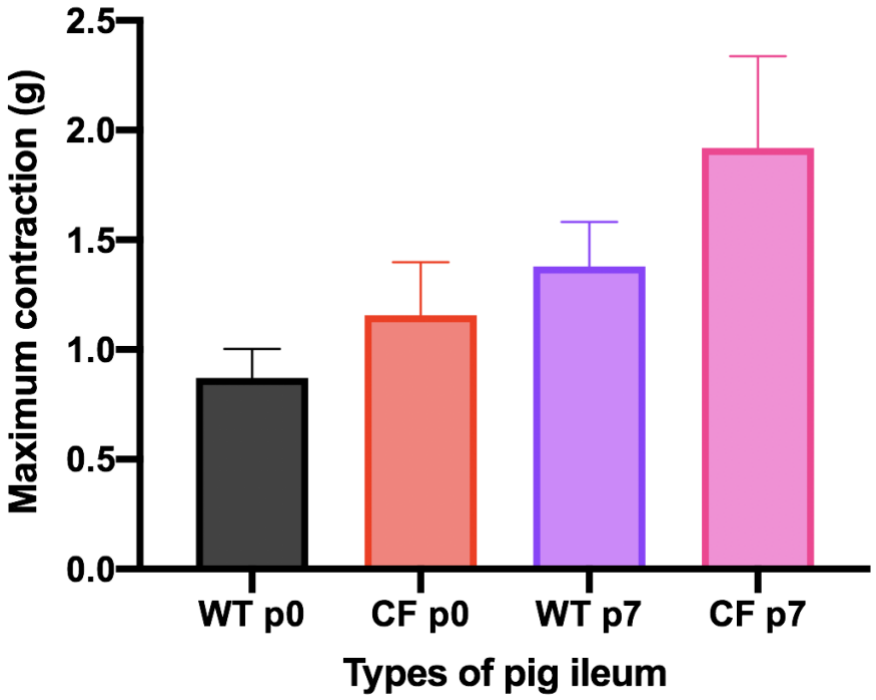

Figure 3-13: The maximum contraction tension induced by histamine in wild-type neonate (WTp0), CFTR$^{-/-}$ neonate (CFp0), wild-type one-week-old (WTp7), CFTR$^{-/-}$ one-week-old (CFp7) swine (WTp0, n= 5 assays from 8 pigs; CFp0, n= 8 assays from 4 animals; WTp7 n= 17 assays from 11 animals; CFp7, n= 3 assays from 2 animals; One-way ANOVA test). Data is presented as mean ± SEM.

3.4.2 Amplitude and Frequency post histamine stimulation

We didn't observe any significant differences in the amplitude and frequency of ileum peristalsis post contraction induced by histamine (*Figure 3-14*).

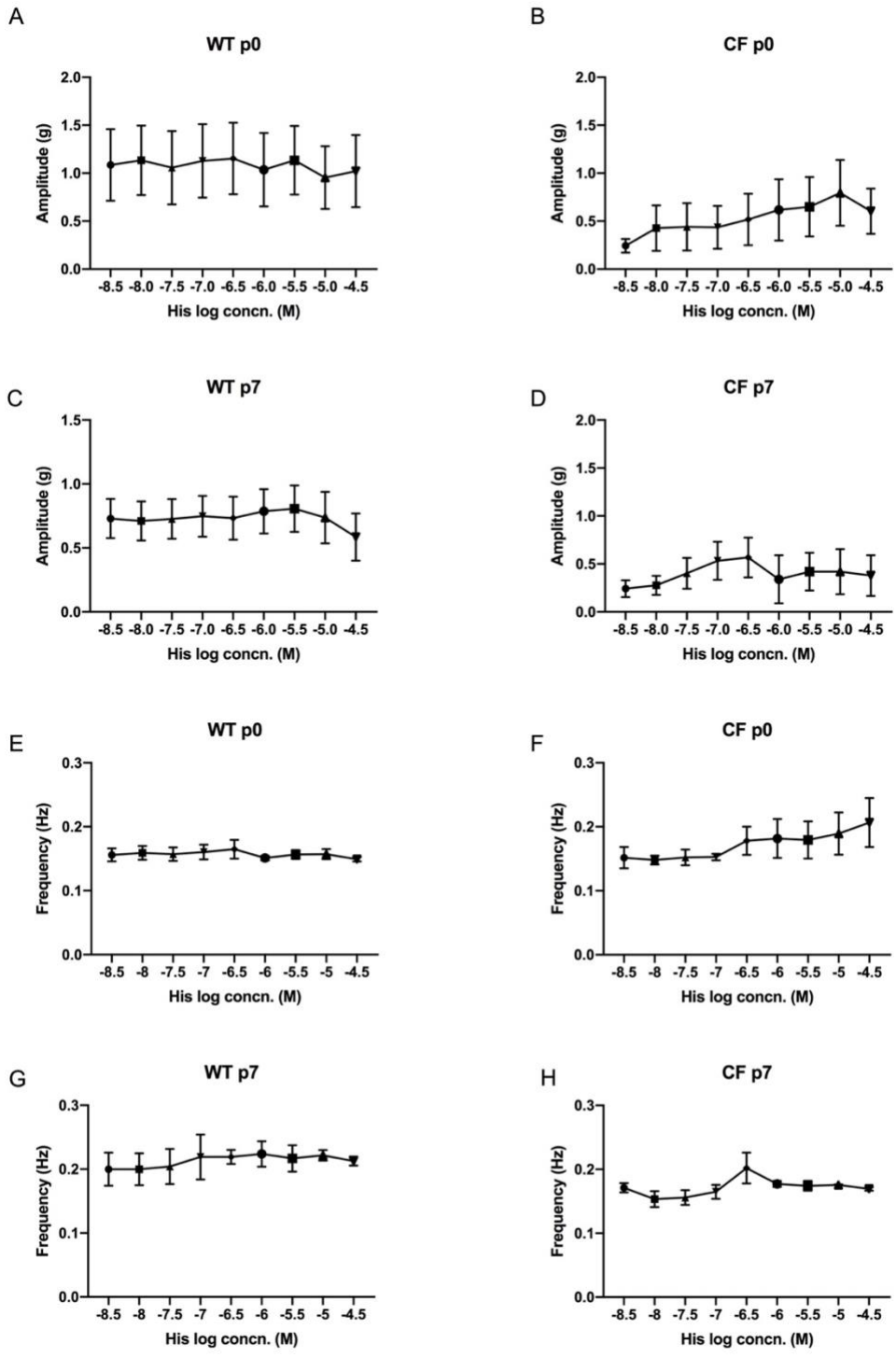

Figure 3-14: Amplitude and frequency of peristaltic waves with increasing concentration of histamine in wild-type neonate (WTp0), CFTR$^{-/-}$ neonate (CFp0), wild-type one-week-old (WTp7), CFTR$^{-/-}$ one-week-old (CFp7) swine (WTp0, n= 5 assays from 8 pigs; CFp0, n= 8 assays from 4 animals; WTp7 n= 17 assays from 11 animals; CFp7, n= 3 assays from 2

animals). A-D) amplitude of peristaltic waves in response to histamine for wild-type p0, CFp0, wild-type p7, and CFp7, respectively. There is no significant difference between each point and the baseline first point. E-H) Frequency of peristaltic waves in response to histamine for wild-type p0, CFp0, wild-type p7, and CFp7, respectively. One-Way ANOVA, data is presented as mean ± SEM.

3.4.3 Effect of cetirizine on histamine dose-response curve

Similar to serotonin dose-response curves, we only performed the experiment using two different concentrations of histamine antagonist cetirizine. We observed that both wild-type tissues and neonate $CFTR^{-/-}$ tissue responded as we were expecting, ie. right-shift of the dose-response curve with increasing concentration of the antagonist (*Figure 3-15 A, B, and C*). However, one-week-old $CFTR^{-/-}$ tissue did not follow this pattern and the EC_{50} value for cetirizine 3µM was larger than that of 1µM (*Figure 3-15 D, Table 3-5*).

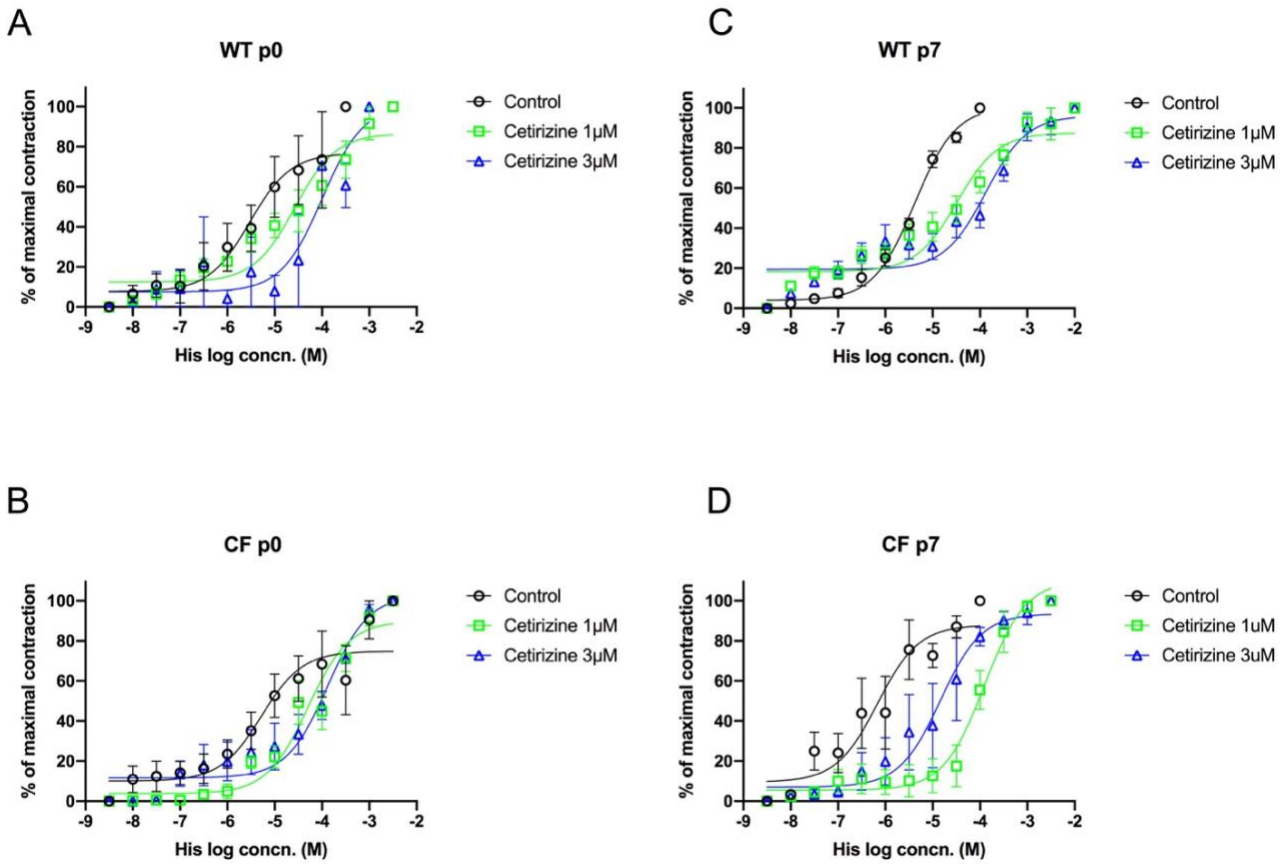

Figure 3-15: Dose-response curve of histamine-induced contraction in the presence of two different concentrations of antagonist cetirizine in wild-type neonate (WTp0), CFTR$^{-/-}$ neonate (CFp0), wild-type one-week-old (WTp7), CFTR$^{-/-}$ one-week-old (CFp7) swine (WTp0, n= 5 assays from 8 pigs; CFp0, n= 8 assays from 4 animals; WTp7 n= 17 assays from 11 animals; CFp7, n= 3 assays from 2 animals). A-D) Dose-response curve of wild-type p0, CFp0, wild-type p7, and CFp7, respectively. For each graph, the curves are significantly different (the Extra sum-of-squares F test). Data is presented as mean ± SEM.

Table 3-6: EC_{50} values of histamine-induced contraction with increasing concentrations of cetirizine.

	Histamine alone (µM)	Histamine + cetirizine 1µM (µM)	Histamine + cetirizine 3µM (µM)
Wild-type neonates	2.95	26.6	101
$CFTR^{-/-}$ neonates	5.24	50.3	131
Wild-type one-week-olds	4.16	32.6	132
$CFTR^{-/-}$ one-week-olds	0.681	124	14.6

CHAPTER 4 DISCUSSIONS AND CONCLUSIONs

4.1 Discussions

With the increasing survival rate of CF patients as treatments become more effective, extrapulmonary diseases are becoming more prevalent in patients. One major extrapulmonary effect is gastrointestinal-related abnormalities. However, there is limited knowledge underpinning our understanding of GI complications in CF [114]. One underexplored hypothesis is that CF patients suffer from diminished gut motility, which leads to an increase in content transit time, chances of constipation, and GI blockage. By comparing motility between CF and wild-type pig's ileum contraction, we try to take a step closer to uncover the causes of CF-related abdominal complications.

4.1.1 CF tissue have diminished basal peristalsis

As mentioned in the background section, smooth muscles tend to have an intrinsic tone and contraction pattern [53]. We were able to observe intrinsic peristaltic waves after the tissues were mounted in the isolated organ bath. After finding out the average amplitude and frequency of the ileum peristalsis wave, we concluded that there is a difference in the amplitude but no differences in the frequency of peristalsis between CF and wild-type tissues. We found that the amplitudes of both wild-type tissues (neonates and one-week-old) were significantly larger than their corresponding CF tissues (neonates and one-week-old). Both frequency and amplitude can affect the intensity of peristalsis. The results suggest that CF ileum has a diminished peristaltic contraction. Thus, as the intestinal peristalsis is very important in moving items forward [40], this finding may indicate that CF individuals may have a longer traffic time for GI content, which might contribute to constipation and the development of more severe obstructions such as DIOS.

We also compared neonate tissue with one-week-old tissue in terms of their peristaltic amplitude and frequency. The reason we decided to compare them is that we wanted to see if there is any improvement in peristalsis as the piglet grows because the piglet's intestinal function improves rapidly during the first week after birth [115]. We found there were no differences in frequency or amplitude as they grow older (between CF neonates and one-week-olds or WT

neonates and one-week-olds). It indicates that the amplitude of peristalsis was determined pre-birth, and the CF animals (neonate and one-week-old) had much smaller amplitude than that of the wild-type.

The frequency of peristalsis is initiated and controlled by the slow waves of the longitudinal muscle, which acts as a pacemaker [54,116]. Since we did not observe any differences in the frequency of peristalsis, it could mean that the pacemaker (or the slow waves of the smooth muscle) is not affected by the CFTR dysfunction. However, CFTR dysfunction likely affected the smooth muscle capacity for contraction in the intestine, which resulted in decreased GI motility amplitude.

4.1.2 Contraction in response to acetylcholine

Cholinergic modulation of GI motility is an important determinant of peristalsis and gut contractions [54]. Treatment with ACh had a stimulatory effect both in CF and wild-type swine ileum preparations. In this section, we discuss ACh-induced contraction, peristalsis, and receptor affinity to its antagonist.

<u>CF tissues have a reduced sensitivity to ACh-induced contraction</u>

We found that all the tissues responded to ACh with an increased contraction compared to the baseline. De Lisle et al, (2010) showed that cholinergic stimulation in mouse small intestine with only the wild-type tissues responded to ACh, while the CF tissues failed to respond [97]. Our results differ from those of De Lisle et al (2010) in that both CF and wild-type swine ileum responded to ACh stimulation. However, wild-type swine ileum tissue had higher sensitivity for ACh (i.e. increased contraction at a lower concentration of ACh, compared to CF tissues). The result indicates that CF tissues have a reduced response to ACh-induced contraction either due to reduced receptor affinity for ACh or because of reduced contractility after stimulation. Furthermore, we also observed that wild-type one-week-old preparations were more sensitive than neonates, while both CF tissues (neonates and one-week-old) had similar sensitivities. This shows that CF tissues' sensitivity to ACh-induced contraction did not improve as the animal aged.

Wildtype one-week-old tissue have a larger maximum ACh-stimulated contraction

Comparing the maximum contraction for each type of tissue induced by ACh, we can reach several conclusions. First, we found that the maximum contraction of CF one-week-old tissue is significantly smaller compared to the wild-type tissue. This finding is consistent with our hypothesis that CF pigs have a reduced ACh-stimulated contraction response than their wild-type counterparts. Second, we found that the wild-type neonate was significantly different than the wild-type one-week-old tissue, which had a much larger maximum contraction, suggesting that the ability of the ileum to contract in response to ACh increases or develops post-birth. Interestingly the basal amplitude of peristalsis didn't change after birth (*Figure 3-1 A*). On the other hand, this postnatal increase in ACh response was not observed in the ileum from CF piglets. CF neonate ileum's maximum contraction in response to ACh is similar to that of the one-week-old CF tissue preparations, but both were significantly smaller than that of the wild-type one-week-old tissues.

One possible explanation for the observation of postnatal changes in ACh response might be that the smooth muscle in the ileum has fully developed basal peristaltic contraction capabilities, and in the first few days of life, it develops the capability to respond to cholinergic stimulation. In CF, the postnatal development of the response to ACh stimulation is diminished. It is possible that older CF animals may eventually fully develop the appropriate response to ACh.

Amplitude and frequency

Stimulation with ACh had a significant effect on the amplitude of the peristaltic movements (*Figure 3-4*). At high concentrations, we saw a decrease in amplitude of peristalsis and a concomitant increase in the tone of muscle contraction. The data suggest that at a high ACh concentration the tissue is unable to relax, and the peristaltic contraction amplitude decreased. However, this effect was less evident in CF tissues, probably since the contraction induced by ACh was not as large. Thus, the muscle tone was more relaxed, and the tissue was

still able to maintain peristaltic contraction amplitude in CF preparations, even at high ACh concentrations. ACh did not affect the peristaltic contraction frequency.

Dose-response curve

We produced a dose-response curve for data normalized to the maximum contraction tension (*Figure 3-6*). The dose-response curves for ACh for all preparations followed the expected trend, i.e. the dose-response curve for ACh shifted to the right as the preparations were incubated with increasing concentration of the antagonist atropine with increasing EC_{50} values. After comparing the four curves on each graph (*Figure 3-6A-D*), we found that a rightward parallel shift of the ACh dose-response curves in the presence of increasing antagonist concentrations indicates competitive antagonism by atropine.

Schild plot

Using the EC_{50} values we graphed the Schild plot. The slope and the x-intercept of the Schild plot can be used to determine some properties of the antagonist atropine on the ACh receptor. The slope of the Schild plot for a competitive antagonist should be -1 [117]. We found that both wild-type and CF neonate tissue preparations had a Schild plot slope very close to -1. However, for the one-week-old tissues, the slopes were different from each other, and they are not as close to -1. This can be a result of smaller sample size and inconsistent data. However, a slope significantly different from -1 may signify that there are multiple receptors (receptor subtypes) expressed in the smooth muscle cells or non-competitive antagonism [113,117].

The pA_2 value is the concentration of the antagonist needed to double the concentration of agonist required to elicit the same response obtained in the absence of the antagonist [110]. pA_2 is a measure of the affinity of the antagonist to the receptor [110]. A larger pA_2 value indicates that atropine has a higher specificity for the muscarinic ACh receptor. In our experiments, all the pA_2 values were very close to each other, around 9. Therefore, we conclude that there are no differences in the affinity of the antagonist to the receptor between genotypes.

We found two other published works comparing intestinal contraction on CF and wild-type mice. As mentioned before, *De Lisle et al*, (2010)'s organ bath studies, similar to what we

have done, measured the contraction by the mouse duodenum. Their results show that wild-type mice small intestine responded to cholinergic agonists while the CF mice tissues did not respond [97]. In contrast, we found that CF pig ileum responded to ACh albeit with significantly diminished sensitivity compared to the wild-type swine. They also measured the amplitude and frequency of the peristaltic wave. They found that wild-type tissue has a more regular phasic contractile behavior. We found that CF tissues have a decreased amplitude of peristalsis, but we were not able to determine the regularity of the peristalsis.

Risse et al. in 2012 used mice ileum tissue to study motility [81]. They used an electric field stimulation of muscle contraction with increasing concentrations of different agonists [81]. One of the cholinergic agonists they used was methacholine. They found that CF mice tissue had a larger force of contraction in response to the agonist compared to the wild-type tissue. Furthermore, they stated that there are no differences between the resting muscle tone for the two types of tissues. Those results are in opposition to what we found, where CF swine ileum had reduced contractility in response to cholinergic stimulation. The difference may be due to the experimental approach or a species difference.

4.1.3 Contraction in response to serotonin and histamine

Compared to ACh, the tissues did not respond well to either serotonin or histamine, and we were not able to obtain sufficient data points for effective analysis. However, with the results we obtained, we can still arrive at some conclusions.

Serotonin

CF one-week-old tissue did not respond to serotonin-induced contraction

The wild-type tissues, both neonate and one-week-old, responded to serotonin with increased peristaltic contraction (*Figure 3-8*). In contrast, CF preparations from one-week-old animals failed to increase the force of contraction in response to serotonin above baseline levels. Newborn CF preparations did respond to serotonin but with lower sensitivity than WT (*Figure 3-8*). We can interpret these results as indicating that with the loss of CFTR function, the ability of the ileum to respond to serotonin decreased and that this complication may be aggravated during post-natal development. However, we also need to consider that the sample size is small, and it

could affect our results especially for the one-week-old CF group that includes four experiments from two piglets.

Maximum contraction and peristalsis

The maximum contraction induced by serotonin was similar in all the experimental groups. It indicates that CFTR dysfunction does not affect serotonin-induced maximum contraction. Furthermore, we did not find any differences in amplitude and frequency when the tissue was stimulated by serotonin. Thus, CFTR dysfunction did not affect serotonin-induced maximum contraction and peristalsis.

Dose-response curve

Lastly, we also graphed the dose-response curve for serotonin-induced normalized contraction. The dose-response curve for the wild-type tissues shifted to the right after exposure to the antagonist, as expected. However, we did not collect sufficient data from CF tissues, and it could not be fitted to a dose-response curve through non-linear regression.

Bubenik (1986) conducted experiments of serotonin's effect on rat ileum and in the presence of the antagonist methysergide [118]. They used an apparatus system similar to the organ bath system. He found that there is a dose-dependent increase in the ileum muscle contraction with reduced amplitude. They also found that the presence of the antagonist methysergide blocks the effect of serotonin on the intestine. We found similar results, but we did not see a reduction in amplitude in the wild-type tissue. Unfortunately, we did not find other research on the effect of serotonin on the CF ileum.

Histamine

Similar to serotonin, histamine-induced contraction did not respond well either, especially for the CF tissues. The analysis we conducted was the same as that for serotonin.

Wildtype responded to histamine-induced contraction

Wild-type tissues had a significant increase in contraction induced by histamine while the CF tissues did not. However, from *Figure 3-12*, the average contraction for CF tissues was higher than that of the wild-type tissues. The cause is that our sample sizes are too small for CF tissues thus making the error bars too large.

Maximum contraction

Similar to serotonin results, we did not find any differences among the tissues for the average maximum contraction, or amplitude and frequency. The CFTR dysfunction likely did not have an impact on histamine-induced max contraction and peristalsis. However, the results could be due to small sample sizes.

Dose-response curve

The dose-response curve for histamine-induced contraction was better compared to that of serotonin. However, the results for the CF tissues were not as expected. With the increasing concentration of the antagonist, the EC_{50} values should have increased with the curve shifting to the right. However, this was not observed in the CF tissues. It could be that the tissues were not able to respond properly to histamine due to CFTR dysfunction or due to the small sample sizes as many tissues stopped responding when the concentration of the antagonist reached its highest.

Summary

In summary, we found that there is a difference in wild-type and CF ileum peristalsis and contraction. Wild-type tissue has a larger peristaltic amplitude compared to CF indicating better GI motility. Wild-type one-week-old tissue also has a bigger maximum contraction tension induced by ACh compared to wild-type neonate and CF tissues. We also observed a decrease in peristaltic amplitude with increasing concentration of ACh in wild-type tissues but not in the CF tissues. The results we found for serotonin- and histamine-induced contraction was less reliable compared to those of ACh due to the limitations of the experiment and the tissue responses.

4.2 Limitations

The main limitation of this study was the amount of $CFTR^{-/-}$ swine tissue available for experimentation. There was only a very limited number of CF piglets available. Dividing them into two separate groups further decreased the sample sizes. Thus, we analyzed the data with the limited sample sizes and obtained results with large error bars.

Serotonin and histamine had even smaller sample sizes compared to those induced by ACh because some tissues did not respond. Also, the concentration of the antagonist was somewhat too high for the tissues, as some tissues stopped responding (completely blocked). Since we conducted the CF experiments first, we could not change the concentration of the antagonist when we discovered the problem. We should have also conducted the experiment with at least three different concentrations of antagonists so that we could have also plotted the Schild plot, but we had a limited amount of CF tissue. Furthermore, for the tissues that did not respond to serotonin or histamine, we should have conducted a positive control using ACh to test whether the tissue was not responding to a specific agonist or whether was not viable or dead. We unfortunately only did this for a few samples but not all. For this experiment, we considered a tissue to be viable if it had consistent peristaltic waves before treatment. With a positive control, it could reinforce the unresponsiveness of the tissue to the specific agonist.

There were also experimental design limitations. The organ bath is effective in measuring changes in muscle movement. However, the apparatus doesn't give any information on the molecular and cellular biology of motility, such as receptor type and quantity. Some researchers have used other techniques, such as gene/protein analysis to compare muscle contraction [119]. Even though we were able to measure some aspects of the receptor's properties using the data collected by the organ bath and the Schild plot, the measurement was indirect.

4.3 Future work

From the result we obtained, we conclude that CFTR gene knockout piglets have a reduced ileal contraction and peristalsis compared to wild-type. The reduced ability of the intestinal smooth muscle was the cause of this effect. De Lisle et al. also found that the defect is

at the smooth muscle level [97]. Thus, for our future works, we want to look in detail at what specific mechanisms/substances are abnormal in the smooth muscle.

First, we want to investigate the contraction of the smooth muscle to see if there are any abnormalities in the smooth muscle contraction. Different from skeletal and cardiac muscle, smooth muscle uses the calcium/calmodulin/MLCK complex to initiate the power stroke for contraction. To test if there is anything wrong with the smooth muscle contraction, we plan to use histology to look into the microscopic level of the smooth muscle. Other authors have suggested that there is muscle hypertrophy/hyperplasia in CF tissues [120]. So, we also want to compare the sizes of the muscle. We will be using frozen wild-type and CF tissues to conduct the histology experiments.

Second, we hypothesize that it could be that the loss of CFTR function in the neurons is affecting muscle contraction. Thus, we also want to measure the neuronal function and potentially go into more detail about testing the receptor properties. We propose to use Western blotting to test the type and quantity of the receptors to complement the Schild plot results reported in this thesis. Other CF researchers have done western blotting to compare intestinal muscle properties, and they found significant results [81].

4.4 Relevance for CF

Our experiments may shed light on the pathobiology of CF patients' intestinal complications. Our results suggest that CF ileum suffers from reduced basal peristaltic motility and reduced response to ACh stimulation. We also found $CFTR^{-/-}$ pig ileum cannot overcome their limited contraction ability through growth as the wild-type ileum up to one week. We propose as a working hypothesis that abnormal motility may contribute to intestinal complications of the CF patients, such as constipation and DIOS. Therapies aimed at increasing GI motility in CF may reduce the incidence of DIOS and constipation.

REFERENCES

1. Lavelle GM, White MM, Browne N, McElvaney NG, Reeves EP. Animal Models of Cystic Fibrosis Pathology: Phenotypic Parallels and Divergences. Gualillo O, ed. *Biomed Res Int*. 2016;2016:5258727. doi:10.1155/2016/5258727
2. Cutting GR. Cystic fibrosis genetics: From molecular understanding to clinical application. *Nat Rev Genet*. 2015. doi:10.1038/nrg3849
3. Tabori H, Arnold C, Jaudszus A, et al. Abdominal symptoms in cystic fibrosis and their relation to genotype, history, clinical and laboratory findings. *PLoS One*. 2017;12(5):1-19. doi:10.1371/journal.pone.0174463
4. Quinton PM. Cystic fibrosis: Lessons from the sweat gland. *Physiology*. 2007;22(3):212-225. doi:10.1152/physiol.00041.2006
5. ANDERSEN DH. Cystic fibrosis of the pancreas and its relation to celiac disease: A clinical and pathologic study. *Am J Dis Child*. 1938;56(2):344-399. doi:10.1001/archpedi.1938.01980140114013
6. Agrons GA, Corse WR, Markowitz RI, Suarez ES, Perry DR. From the Archives of the AFIP Gastrointestinal Manifestations of Cystic Fibrosis: Radiologic-Pathologic Correlation. *Radiographics*. 1996;16(4):871-893. doi:10.1148/radiographics.16.4.8835977
7. Davis PB. Cystic fibrosis since 1938. *Am J Respir Crit Care Med*. 2006;173(5):475-482. doi:10.1164/rccm.200505-840OE
8. Di Sant'Agnese PA, Darling RC, Perera GA, Shea E. Abnormal electrolyte composition of sweat in cystic fibrosis of the pancreas. *Pediatrics*. 1953;12:549-563.
9. Quinton PM. Chloride impermeability in cystic fibrosis. *Nature*. 1983;301(5899):421-422. doi:10.1038/301421a0
10. Riordan JR, Rommens JM, Kerem BS, et al. Identification of the cystic fibrosis gene: Cloning and characterization of complementary DNA. *Science (80-)*. 1989;245(4922):1066-1073. doi:10.1126/science.2475911
11. Kerem BS. Identification of the cystic fibrosis gene: genetic analysis. *Trends Genet*. 1989;5(C):363. doi:10.1016/0168-9525(89)90156-X
12. Zaher A, ElSaygh J, Elsori D, ElSaygh H, Sanni A. A Review of Trikafta: Triple Cystic Fibrosis Transmembrane Conductance Regulator (CFTR) Modulator Therapy. *Cureus*. 2021;13(7):e16144. doi:10.7759/cureus.16144

13. Stephenson AL, Sykes J, Stanojevic S, et al. Survival comparison of patients with cystic fibrosis in Canada and the United States: a population-based cohort study. *Physiol Behav*. 2017;166(8):537-546. doi:10.1016/j.physbeh.2017.03.040
14. Reznikov LR. Cystic Fibrosis and the Nervous System. *Chest*. 2017;151(5):1147-1155. doi:10.1016/j.chest.2016.11.009
15. Bell SC, Mall MA, Gutierrez H, et al. The future of cystic fibrosis care: a global perspective. *Lancet Respir Med*. 2019;0(0). doi:10.1016/S2213-2600(19)30337-6
16. Meng X, Clews J, Martin ER, Ciuta AD, Ford RC. The structural basis of cystic fibrosis. *Biochem Soc Trans*. 2018;46(5):1093-1098. doi:10.1042/BST20180296
17. Bulley S, Jaggar JH. Cl - channels in smooth muscle cells. *Pflugers Arch Eur J Physiol*. 2014;466(5):861-872. doi:10.1007/s00424-013-1357-2
18. Cant N, Pollock N, Ford RC. CFTR structure and cystic fibrosis. *Int J Biochem Cell Biol*. 2014;52:15-25. doi:10.1016/j.biocel.2014.02.004
19. Thiagarajah JR, Verkman AS. CFTR pharmacology and its role in intestinal fluid secretion. *Curr Opin Pharmacol*. 2003;3(6):594-599. doi:10.1016/j.coph.2003.06.012
20. Csanády L, Vergani P, Gadsby DC. STRUCTURE, GATING, AND REGULATION OF THE CFTR ANION CHANNEL. *Physiol Rev*. 2019. doi:10.1152/physrev.00007.2018
21. Sheppard DN, Welsh MJ. Structure and function of the CFTR chloride channel. *Physiol Rev*. 1999;79(1 SUPPL. 1):23-45. doi:10.1152/physrev.1999.79.1.S23
22. Chappe V, Hinkson DA, Zhu T, Chang XB, Riordan JR, Hanrahan JW. Phosphorylation of protein kinase C sites in NBD1 and the R domain control CFTR channel activation by PKA. *J Physiol*. 2003;548(1):39-52. doi:10.1113/jphysiol.2002.035790
23. Patrick AE, Thomas PJ. Development of CFTR structure. *Front Pharmacol*. 2012;3 SEP(September):1-11. doi:10.3389/fphar.2012.00162
24. Saint-Criq V, Gray MA. Role of CFTR in epithelial physiology. *Cell Mol Life Sci*. 2017;74(1):93-115. doi:10.1007/s00018-016-2391-y
25. Borowitz D. CFTR, bicarbonate, and the pathophysiology of cystic fibrosis. *Pediatr Pulmonol*. 2015;50(May):S24-S30. doi:10.1002/ppul.23247
26. Veit G, Avramescu RG, Chiang AN, et al. From CFTR biology toward combinatorial pharmacotherapy: Expanded classification of cystic fibrosis mutations. *Mol Biol Cell*. 2016;27(3):424-433. doi:10.1091/mbc.E14-04-0935

27. Fanen P, Wohlhuter-Haddad A, Hinzpeter A. Genetics of cystic fibrosis: CFTR mutation classifications toward genotype-based CF therapies. *Int J Biochem Cell Biol*. 2014;52:94-102. doi:10.1016/j.biocel.2014.02.023
28. Jensen TJ, Loo MA, Pind S, Williams DB, Goldberg AL, Riordan JR. Multiple proteolytic systems, including the proteasome, contribute to CFTR processing. *Cell*. 1995;83(1):129-135. doi:10.1016/0092-8674(95)90241-4
29. Meng X, Clews J, Kargas V, Wang X, Ford RC. The cystic fibrosis transmembrane conductance regulator (CFTR) and its stability. *Cell Mol Life Sci*. 2017;74(1):23-38. doi:10.1007/s00018-016-2386-8
30. Bobadilla JL, Macek M, Fine JP, Farrell PM. Cystic fibrosis: A worldwide analysis of CFTR mutations - Correlation with incidence data and application to screening. *Hum Mutat*. 2002;19(6):575-606. doi:10.1002/humu.10041
31. Yan Z, Stewart ZA, Sinn PL, et al. Ferret and pig models of cystic fibrosis: prospects and promise for gene therapy. *Hum Gene Ther Clin Dev*. 2015;26(1):38-49. doi:10.1089/humc.2014.154
32. Anderson MP, Welsh MJ. Channels Contain Nucleotide-Binding. 1992;257(September):1701-1704.
33. Reddy MRM, Quinton PM. Selective activation of cystic fibrosis transmembrane conductance regulator Cl- and HCO3- conductances. *J Pancreas*. 2001;2(4):212-218.
34. Robertson MB, Choe KA, Joseph PM. Review of the abdominal manifestations of cystic fibrosis in the adult patient. *Radiographics*. 2006;26(3):679-690. doi:10.1148/rg.263055101
35. van Mourik IDM. Liver disease in cystic fibrosis. *Paediatr Child Heal (United Kingdom)*. 2017;27(12):552-555. doi:10.1016/j.paed.2017.07.010
36. Reznikov LR, Dong Q, Chen JH, et al. CFTR-deficient pigs display peripheral nervous system defects at birth. *Proc Natl Acad Sci U S A*. 2013;110(8):3083-3088. doi:10.1073/pnas.1222729110
37. O'Riordan JI, Hayes J, Fitzgerald MX, Redmond J. Peripheral nerve dysfunction in adult patients with cystic fibrosis. *Ir J Med Sci*. 1995. doi:10.1007/BF02967830
38. Chakrabarty B, Kabra SK, Gulati S, et al. Peripheral neuropathy in cystic fibrosis: A prevalence study. *J Cyst Fibros*. 2013;12(6):754-760. doi:10.1016/j.jcf.2013.01.005

39. Boeckxstaens G, Camilleri M, Sifrim D, et al. Fundamentals of neurogastroenterology: Physiology/motility - Sensation. *Gastroenterology*. 2016;150(6):1292-1304.e2. doi:10.1053/j.gastro.2016.02.030
40. Cimino MA, Johnson KK, Michienzi KA. *Gastrointestinal Pharmacology*.; 2006. doi:10.1016/B978-032301808-1.50083-3
41. Furness JB. The enteric nervous system and neurogastroenterology. *Nat Rev Gastroenterol Hepatol*. 2012;9(5):286-294. doi:10.1038/nrgastro.2012.32
42. Xue R, Gu H, Qiu Y, et al. Expression of Cystic Fibrosis Transmembrane Conductance Regulator in Ganglia of Human Gastrointestinal Tract. *Sci Rep*. 2016;6(March):1-8. doi:10.1038/srep30926
43. Hansen MB. Small intestinal manometry. *Physiol Res*. 2002;51(6):541-556.
44. Sanders KM, Kito Y, Hwang SJ, Ward SM. Regulation of gastrointestinal smooth muscle function by interstitial cells. *Physiology*. 2016;31(5):316-326. doi:10.1152/physiol.00006.2016
45. Borysova L, Dora KA, Garland CJ, Burdyga T. Smooth muscle gap-junctions allow propagation of intercellular Ca2+ waves and vasoconstriction due to Ca2+ based action potentials in rat mesenteric resistance arteries. *Cell Calcium*. 2018;75(June):21-29. doi:10.1016/j.ceca.2018.08.001
46. Sanders KM, Koh SD, Ro S, Ward SM. Regulation of gastrointestinal motility—insights from smooth muscle biology Kenton. *Nat Rev Gastroenterol Hepatol*. 2012;9(11):633-645. doi:10.1201/b11479-5
47. Feher J. Intestinal and Colonic Chemoreception and Motility. In: *Quantitative Human Physiology*. Elsevier; 2017:796-809. doi:10.1016/b978-0-12-800883-6.00079-3
48. Bitar KN. Function of gastrointestinal smooth muscle: From signaling to contractile proteins. *Am J Med*. 2003;115(3 SUPPL. 1):15-23. doi:10.1016/S0002-9343(03)00189-X
49. Zhang L, Horowitz B, Buxton ILO. Muscarinic receptors in canine colonic circular smooth muscle. I. Coexistence of M2 and M3 subtypes. *Mol Pharmacol*. 1991;40(6):943-951.
50. Sanders KM. Invited Review: Mechanisms of calcium handling in smooth muscles. *J Appl Physiol*. 2001;91(3):1438-1449. doi:10.1152/jappl.2001.91.3.1438
51. Wray S, Burdyga T. Sarcoplasmic reticulum function in smooth muscle. *Physiol Rev*.

2010;90(1):113-178. doi:10.1152/physrev.00018.2008

52. Horowitz A, Menice CB, Laporte R, Morgan KG. Mechanisms of smooth muscle contraction. *Physiol Rev*. 1996;76(4):967-1003. doi:10.1152/physrev.1996.76.4.967
53. Webb RC. Smooth muscle contraction and relaxation. *Am J Physiol - Adv Physiol Educ*. 2003;27(1-4):201-206. doi:10.1152/advan.00025.2003
54. Montgomery LEA, Tansey EA, Johnson CD, Roe SM, Quinn JG. Autonomic modification of intestinal smooth muscle contractility. *Adv Physiol Educ*. 2016;40(1):104-109. doi:10.1152/advan.00038.2015
55. Garza A, Huang LZ, Son J-H, Winzer-Serhan UH. Expression of nicotinic acetylcholine receptors and subunit messenger RNAs in the enteric nervous system of the neonatal rat. *Neuroscience*. 2009;158(4):1521-1529. doi:10.1038/jid.2014.371
56. Spencer NJ, Hu H. Enteric nervous system: sensory transduction, neural circuits and gastrointestinal motility. *Nat Rev Gastroenterol Hepatol*. 2020;17(6):338-351. doi:10.1038/s41575-020-0271-2
57. Wikberg J. Localization of Adrenergic Receptors in Guinea Pig Ileum and Rabbit Jejunum to Cholinergic Neurons and to Smooth Muscle Cells. *Acta Physiol Scand*. 1977. doi:10.1111/j.1748-1716.1977.tb10370.x
58. Srinivasan BGN and S. Enteric Nervous System in the Small Intestine: Pathophysiology and Clinical Implications. *Curr Gastroenterol Rep*. 2012;23(1):1-7. doi:10.1007/s11894-010-0129-9.Enteric
59. Yau WM. Effect of substance P on intestinal muscle. *Gastroenterology*. 1978;74(2 PART 1):228-231. doi:10.1016/0016-5085(78)90802-8
60. Kitazawa T, Kaiya H. Regulation of gastrointestinal motility by motilin and ghrelin in vertebrates. *Front Endocrinol (Lausanne)*. 2019;10(MAY):1-17. doi:10.3389/fendo.2019.00278
61. Chandra R, Liddle RA. Cholecystokinin. 2007:63-67.
62. Iwasaki M, Akiba Y, Kaunitz JD. Recent advances in vasoactive intestinal peptide physiology and pathophysiology: Focus on the gastrointestinal system [version 1; peer review: 4 approved]. *F1000Research*. 2019;8:1-13. doi:10.12688/f1000research.18039.1
63. Lelievre V, Favrais G, Abad C, et al. Gastrointestinal dysfunction in mice with a targeted mutation in the gene encoding vasoactive intestinal polypeptide: A model for the study of

intestinal ileus and Hirschsprung's disease. *Peptides*. 2007;28(9):1688-1699. doi:10.1016/j.peptides.2007.05.006

64. Makhlouf GM, Murthy KS. Signal Transduction in Gastrointestinal Smooth Muscle. *Cell Signal*. 1997;9(3-4):269-276. doi:10.1016/S0898-6568(96)00180-5
65. Brown DA. Acetylcholine and cholinergic receptors. *Brain Neurosci Adv*. 2019;3:239821281882050. doi:10.1177/2398212818820506
66. Whalen K, Finkel R, Panavelil TA. *Lippincott Illustrated Reviews: Pharmacology*.; 2015. doi:10.1017/CBO9781107415324.004
67. Kuo IY, Ehrlich BE. Signaling in muscle contraction. *Cold Spring Harb Perspect Biol*. 2015;7(2). doi:10.1101/cshperspect.a006023
68. Iino S, Nojyo Y. Muscarinic M2 acetylcholine receptor distribution in the guinea-pig gastrointestinal tract. *Neuroscience*. 2006;138(2):549-559. doi:10.1016/j.neuroscience.2005.11.021
69. Bolton TB, Lim SP. Action of acetylcholine on smooth muscle. In: *Zeitschrift Fur Kardiologie*. ; 1991.
70. Muise ED, Gandotra N, Tackett JJ, Bamdad MC, Cowles RA. Distribution of muscarinic acetylcholine receptor subtypes in the murine small intestine. *Life Sci*. 2017;169:6-10. doi:10.1016/j.lfs.2016.10.030
71. Banskota S, Ghia JE, Khan WI. Serotonin in the gut: Blessing or a curse. *Biochimie*. 2019;161:56-64. doi:10.1016/j.biochi.2018.06.008
72. Mawe GM, Hoffman JM. Serotonin signalling in the gut-functions, dysfunctions and therapeutic targets. *Nat Rev Gastroenterol Hepatol*. 2013;10(8):473-486. doi:10.1038/nrgastro.2013.105
73. Spohn SN, Mawe GM. Non-conventional features of peripheral serotonin signalling-the gut and beyond. *Nat Rev Gastroenterol Hepatol*. 2017;14(7):412-420. doi:10.1038/nrgastro.2017.51
74. Tuladhar BR, Ge L, Naylor RJ. 5-HT 7 receptors mediate the inhibitory effect of 5-HT on peristalsis in the isolated guinea-pig ileum. *Br J Pharmacol*. 2003;138(7):1210-1214. doi:10.1038/sj.bjp.0705184
75. COSTA M, FURNESS JB. The Sites of Action of 5-Hydroxytryptamine in Nerve-Muscle Preparations From the Guinea-Pig Small Intestine and Colon. *Br J Pharmacol*.

1979;65(2):237-248. doi:10.1111/j.1476-5381.1979.tb07824.x

76. Lördal M, Hellström PM. Serotonin stimulates migrating myoelectric complex via 5-HT3-receptors dependent on cholinergic pathways in rat small intestine. *Neurogastroenterol Motil*. 1999;11(1):1-10. doi:10.1046/j.1365-2982.1999.00125.x
77. Sullivant A, Mackin A, Pharr T, Cooley J, Wills R, Archer T. Identification of histamine receptors in the canine gastrointestinal tract. *Vet Immunol Immunopathol*. 2016. doi:10.1016/j.vetimm.2016.09.010
78. Sander LE, Lorentz A, Sellge G, et al. Selective expression of histamine receptors H1R, H2R, and H4R, but not H3R, in the human intestinal tract. *Gut*. 2006;55(4):498-504. doi:10.1136/gut.2004.061762
79. Peters LJ, Kovacic JP. Histamine: metabolism, physiology, and pathophysiology with applications in veterinary medicine. *J Vet Emerg Crit Care*. 2009;19(4):311-328. doi:10.1111/j.1476-4431.2009.00434.x
80. Michoud MC, Robert R, Hassan M, et al. Role of the cystic fibrosis transmembrane conductance channel in human airway smooth muscle. *Am J Respir Cell Mol Biol*. 2009;40(2):217-222. doi:10.1165/rcmb.2006-0444OC
81. Risse PA, Kachmar L, Matusovsky OS, et al. Ileal smooth muscle dysfunction and remodeling in cystic fibrosis. *Am J Physiol - Gastrointest Liver Physiol*. 2012;303(1):1-8. doi:10.1152/ajpgi.00356.2011
82. De Lisle RC, Meldi L, Mueller R. Intestinal Smooth Muscle Dysfunction Develops Postnatally in Cystic Fibrosis Mice. *J Pediatr Gastroenterol Nutr*. 2012;55(6):689-694. doi:10.1097/MPG.0b013e3182638bf4
83. Stoltz DA, Rokhlina T, Ernst SE, et al. Intestinal CFTR expression alleviates meconium ileus in cystic fibrosis pigs. *J Clin Invest*. 2013;123(6):2685-2693. doi:10.1172/JCI68867
84. Rogers CS, Stoltz DA, Meyerholz DK, et al. Disruption of the CFTR gene produces a model of cystic fibrosis in newborn pigs. *Science (80-)*. 2008;321(5897):1837-1841. doi:10.1126/science.1163600
85. Ooi CY, Durie PR. Cystic fibrosis from the gastroenterologist's perspective. *Nat Rev Gastroenterol Hepatol*. 2016;13(3):175-185. doi:10.1038/nrgastro.2015.226
86. Ciprandi G, Rivosecchi M. Meconium ileus. *Newborn Surgery, Fourth Ed*. 2017:618-623. doi:10.4324/9781315113968

87. De Lisle RC, Borowitz D. The cystic fibrosis intestine. *Cold Spring Harb Perspect Med*. 2013;3(9):1-18. doi:10.1101/cshperspect.a009753
88. Houwen RH, Van Der Doef HP, Sermet I, et al. Defining DIOS and constipation in cystic fibrosis with a multicentre study on the incidence, characteristics, and treatment of DIOS. *J Pediatr Gastroenterol Nutr*. 2010;50(1):38-42. doi:10.1097/MPG.0b013e3181a6e01d
89. Van Der Doef HPJ, Kokke FTM, Van Der Ent CK, Houwen RHJ. Intestinal obstruction syndromes in cystic fibrosis: Meconium ileus, distal intestinal obstruction syndrome, and constipation. *Curr Gastroenterol Rep*. 2011;13(3):265-270. doi:10.1007/s11894-011-0185-9
90. van der Doef HPJ, Kokke FTM, Beek FJA, Woestenenk JW, Froeling SP, Houwen RHJ. Constipation in pediatric Cystic Fibrosis patients: An underestimated medical condition. *J Cyst Fibros*. 2010;9(1):59-63. doi:10.1016/j.jcf.2009.11.003
91. Bali A, Stableforth DE, Asquith P. Prolonged small-intestinal transit time in cystic fibrosis. *Br Med J*. 1983;287(6398):1011-1013.
92. Henen S, Denton C, Teckman J, Borowitz D, Patel D. Review of Gastrointestinal Motility in Cystic Fibrosis. *J Cyst Fibros*. 2021;20(4):578-585. doi:10.1016/j.jcf.2021.05.016
93. Grubb BR, Gabriel SE. Intestinal physiology and pathology in gene-targeted mouse models of cystic fibrosis. *Am J Physiol - Gastrointest Liver Physiol*. 1997;273(2 36-2). doi:10.1152/ajpgi.1997.273.2.g258
94. Dorsey J, Gonska T. Bacterial overgrowth, dysbiosis, inflammation, and dysmotility in the Cystic Fibrosis intestine. *J Cyst Fibros*. 2017;16:S14-S23. doi:10.1016/j.jcf.2017.07.014
95. Hoffman LR, Pope CE, Hayden HS, et al. Escherichia coli dysbiosis correlates with gastrointestinal dysfunction in children with cystic fibrosis. *Clin Infect Dis*. 2014;58(3):396-399. doi:10.1093/cid/cit715
96. Debyser G, Mesuere B, Clement L, et al. Faecal proteomics: A tool to investigate dysbiosis and inflammation in patients with cystic fibrosis. *J Cyst Fibros*. 2016;15(2):242-250. doi:10.1016/j.jcf.2015.08.003
97. De Lisle RC, Sewell R, Meldi L. Enteric circular muscle dysfunction in the cystic fibrosis mouse small intestine. *Neurogastroenterol Motil*. 2010;22(3). doi:10.1111/j.1365-2982.2009.01418.x
98. Yeh KM, Johansson O, Le H, et al. Cystic fibrosis transmembrane conductance regulator

modulates enteric cholinergic activities and is abnormally expressed in the enteric ganglia of patients with slow transit constipation. *J Gastroenterol*. 2019. doi:10.1007/s00535-019-01610-9

99. Hedsund C, Gregersen T, Joensson IM, Olesen HV, Krogh K. Gastrointestinal transit times and motility in patients with cystic fibrosis. *Scand J Gastroenterol*. 2012;47(8-9):920-926. doi:10.3109/00365521.2012.699548
100. Rosen BH, Chanson M, Gawenis LR, et al. Animal and model systems for studying cystic fibrosis. *J Cyst Fibros*. 2018. doi:10.1016/j.jcf.2017.09.001
101. Snouwaert JN, Brigman KK, Latour AM, et al. An animal model for cystic fibrosis made by gene targeting. *Science (80-)*. 1992. doi:10.1126/science.257.5073.1083
102. Semaniakou A, Croll RP, Chappe V. Animal models in the pathophysiology of cystic fibrosis. *Front Pharmacol*. 2019;9(JAN):1-16. doi:10.3389/fphar.2018.01475
103. Welsh MJ, Rogers CS, Stoltz DA, Meyerholz DK, Prather RS. Development of a porcine model of cystic fibrosis. *Trans Am Clin Climatol Assoc*. 2009;120:149-162.
104. Rogers CS, Hao Y, Rokhlina T, et al. Production of CFTR-null and CFTR-ΔF508 heterozygous pigs by adeno-associated virus - Mediated gene targeting and somatic cell nuclear transfer. *J Clin Invest*. 2008;118(4):1571-1577. doi:10.1172/JCI34773
105. Rieger J. The Intestinal Mucosal Network in the Pig: A Histological View on Nutrition-Microbiota-Pathogen-Host-Interactions. 2016.
106. Luan X, Belev G, Tam JS, et al. Cystic fibrosis swine fail to secrete airway surface liquid in response to inhalation of pathogens. *Nat Commun*. 2017;8(1). doi:10.1038/s41467-017-00835-7
107. Barszcz M, Skomiał J. The development of the small intestine of piglets - Chosen aspects. *J Anim Feed Sci*. 2011;20(1):3-15. doi:10.22358/jafs/66152/2011
108. Pleuvry BJ. Receptors, agonists and antagonists. *Anaesth Intensive Care Med*. 2004;5(10):350-352. doi:10.1383/anes.5.10.350.52312
109. Pöch G, Brunner F, Kühberger E. Construction of antagonist dose-response curves for estimation of pA2-values by Schild-plot analysis and detection of allosteric interactions. *Br J Pharmacol*. 1992;106(3):710-716. doi:10.1111/j.1476-5381.1992.tb14399.x
110. ARUNLAKSHANA O, SCHILD HO. Some Quantitative Uses of Drug Antagonists. *Br J Pharmacol Chemother*. 1959;14(1):48-58. doi:10.1111/j.1476-5381.1959.tb00928.x

111. Flacke W, Yeoh TS. Differentiation of acetylcholine and succinylcholine receptors in leech muscle. *Br J Pharmacol Chemother*. 1968;33(1):154-161. doi:10.1111/j.1476-5381.1968.tb00483.x
112. Wyllie DJA, Chen PE. Taking the time to study competitive antagonism. *Br J Pharmacol*. 2007;150(5):541-551. doi:10.1038/sj.bjp.0706997
113. Belz GG. Angiotensin II dose-effect curves and Schild regression plots for characterization of different angiotensin II AT1 receptor antagonists in clinical pharmacology. *Br J Clin Pharmacol*. 2003;56(1):3-10. doi:10.1046/j.1365-2125.2003.01880.x
114. Marsh RJ, Ng C, Major G, Rivett DW, Smyth A, van der Gast CJ. Persistent intestinal abnormalities and symptoms in cystic fibrosis: The underpinning mechanisms impacting gut health and motility. Protocol for a systematic review. *medRxiv*. 2021:2020.07.13.20144808. http://medrxiv.org/content/early/2021/03/16/2020.07.13.20144808.abstract.
115. Skrzypek T., Valverde Piedra J.L., Skrzypek H., Woliński J., Kazimierczak W., Szymańczyk S., Pawłowska M. ZR. Light and scanning electron microscopy evaluation of the postnatal small intestinal mucosa development in pigs. *J Physiol Pharmacol*. 2005;56(supp3):71-87. doi:10.1093/oxfordjournals.annonc.a057902
116. Baker RD. Electrical activity of small intestinal smooth muscle. *Am J Surg*. 1969;117(6):781-797. doi:10.1016/0002-9610(69)90067-1
117. Williams SH, Constanti A. A quantitative study of the effects of some muscarinic antagonists on the guinea-pig olfactory cortex slice. *Br J Pharmacol*. 1988;93(4):855-862. doi:10.1111/j.1476-5381.1988.tb11472.x
118. Bubenik GA. The Effect of Serotonin, N-Acetylserotonin, and Melatonin on Spontaneous Contractions of Isolated Rat Intestine. *J Pineal Res*. 1986;3(1):41-54. doi:10.1111/j.1600-079X.1986.tb00725.x
119. Cook DP, Adam RJ, Zarei K, et al. CF airway smooth muscle transcriptome reveals a role for PYK2. *JCI insight*. 2017;2(17):1-14. doi:10.1172/jci.insight.95332
120. Meyerholz DK, Stoltz DA, Pezzulo AA, Welsh MJ. Pathology of gastrointestinal organs in a porcine model of cystic fibrosis. *Am J Pathol*. 2010;176(3):1377-1389. doi:10.2353/ajpath.2010.090849